Neuroscience week 2021

fnrs
LA LIBERTÉ DE CHERCHER

Biomarkers in Alzheimer's Disease and FrontoTemporal Dementia

E. Salmon, MD, PhD

LIÈGE université
GIGA institute

CYCLOTRON RESEARCH CENTRE
IN VIVO IMAGING

Cyclotron
research centre

Psychologie & Neuroscience Cognitives
PsyNCog
Psychology & Neuroscience of Cognition

Pathological hypotheses in AD

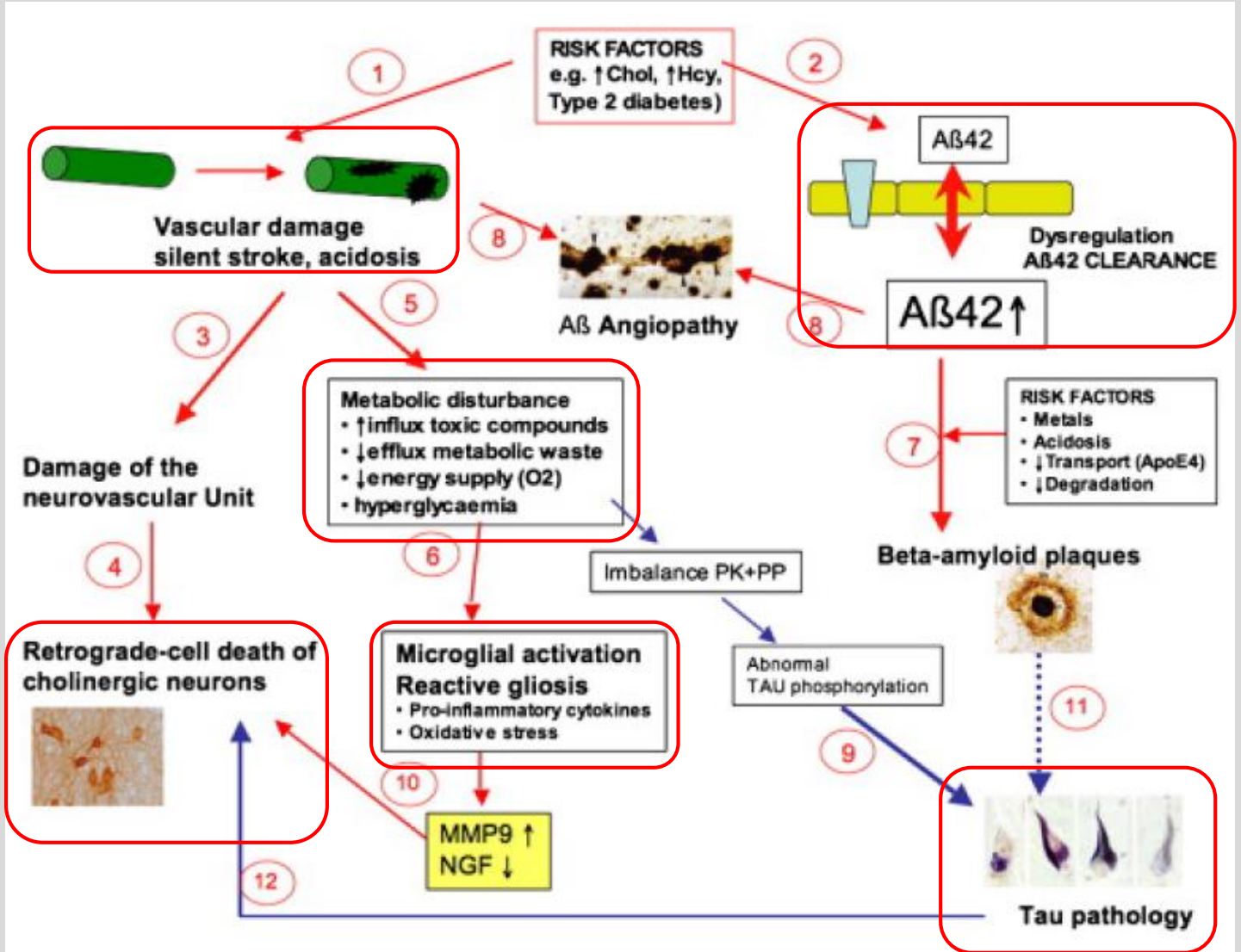

Mice with AD pathology

APP-BASED MOUSE MODELS OF AD		
Tg2576	APP mutation: Swedish	• Intraneuronal Abeta (1.5 m) • Inflammation (2 m) • Memory deficits (4 m) • Synaptic dysfunction (4 m) • Plaques (11 m)
APP AND PSEN DOUBLE TRANSGENIC MICE		
TASTPM	• APP mutation: Swedish • PSEN1 mutation: M146V	• Plaques (6 m) • Inflammation (6 m) • Memory deficits (6 m)
APP/PS1	• APP mutation: Swedish • PSEN1 mutation: deltaE9	• Plaques (6 m) • Inflammation (3 m) • Synaptic dysfunction (4 m) • Memory deficits (12 m) • Neuron loss (8 m)
APPPS1-21	• APP mutation: Swedish • PSEN1 mutation: L166P	• Plaques (1.5 m) • Phosphorylated tau, no mature tangles • Neuron loss (17 m) • Inflammation (1.5 m)
APP/PS2	• APP mutation: Swedish • PSEN2 mutation: N141I	• Plaques (6 m) • Inflammation (6 m) • Synaptic dysfunction (10 m) • Memory deficits (8 m)
5XFAD	• APP mutation: Swedish, Florida, London • PSEN1 mutation: PSEN1, L286V	• Plaques (1.5 m) • Synaptic dysfunction (4 m) • Neuron loss (9 m) • Inflammation (2 m) • Memory deficits (4 m) • Intraneuronal Abeta (1.5 m)

APP, PSEN AND TAU TRANSGENIC MICE		
3xTg	• APP mutation: Swedish • PSEN1 mutation: M146V • Tau mutation: MAPT P301L	• Plaques (6 m) • Tau pathology (12 m) • Intraneuronal Abeta (3 m) • Synaptic dysfunction (6 m) • Memory deficits (4 m) • Inflammation (7 m)
PLB1 Triple	• APP mutation: Swedish, London • PSEN1 mutation: A246E • Tau mutation: MAPT P301L, R406W	• Plaques (21 m) • Hyperphosphorylated tau (6 m) • Intraneuronal Abeta (12 m) • Synaptic dysfunction (12 m) • Memory deficits (12 m) • Inflammation (12 m)
NON-APP-BASED MODEL		
Tg4-42	Overexpressing Aβ4-42 (no mutation)	• Neuron loss (5 m) • Synaptic dysfunction (2 m) • Memory deficits (5 m) • Inflammation (2 m) • Intraneuronal Abeta (2 m)

Positron Emission Tomography

Cerebral metabolism at rest (FDG-PET)

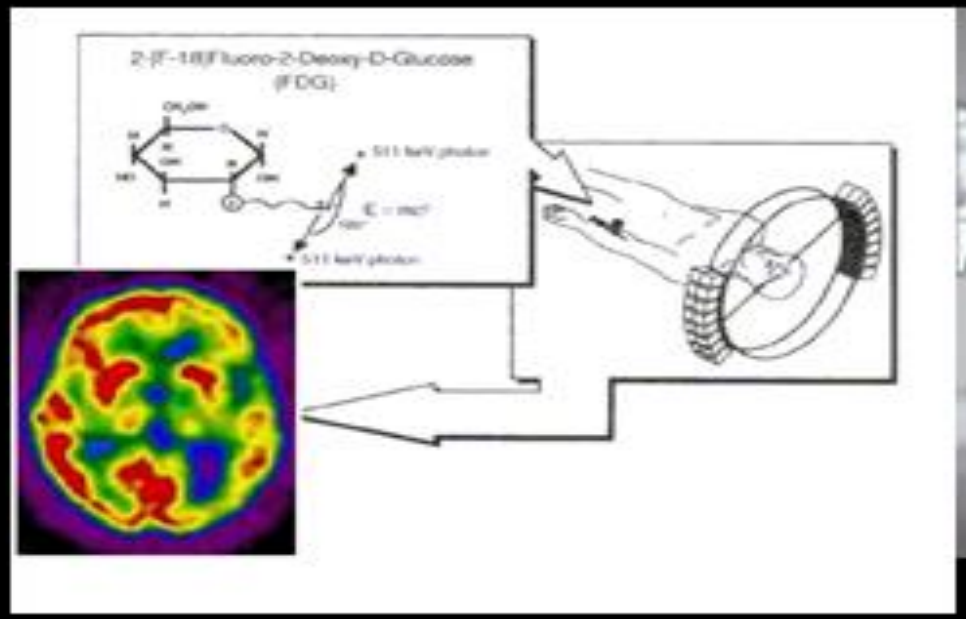

SPM: align, normalize, analyse

18F
11C
15O ($H_2{}^{15}O$)

Positron Emission Tomography

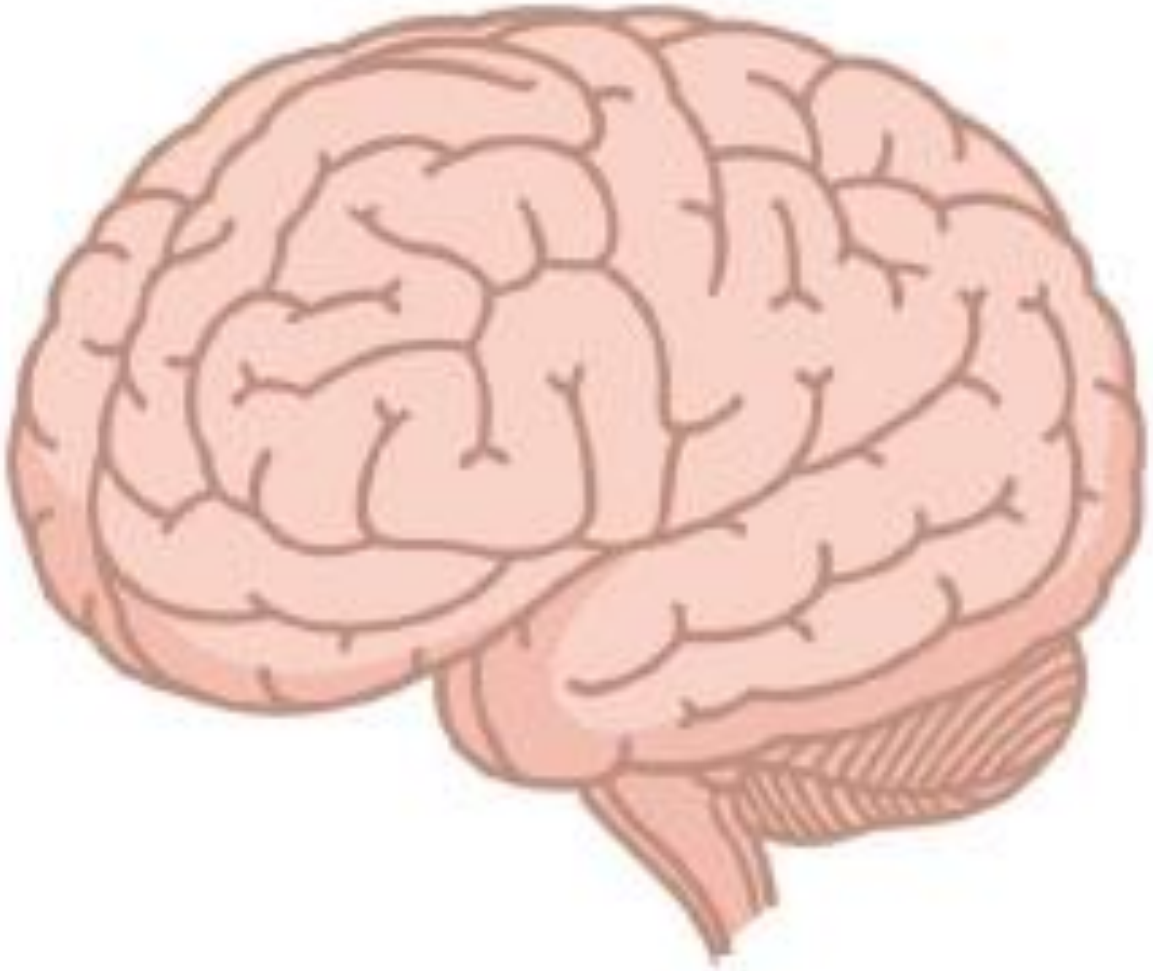

Rat: Factor ~ 600

Mouse: Factor ~ 2400

Positron Emission Tomography in rat

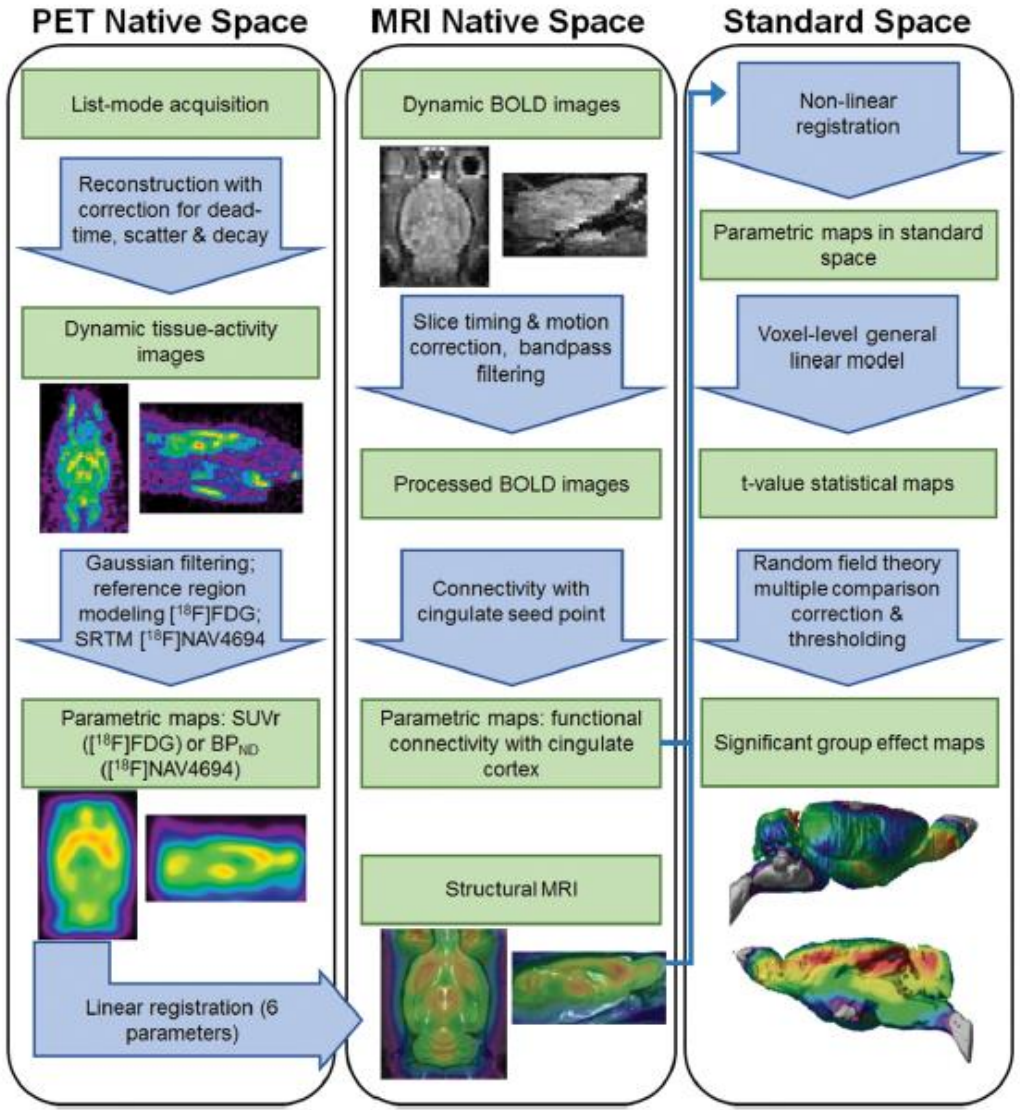

Decreased metabolism in PCC demonstrated by FDG-PET

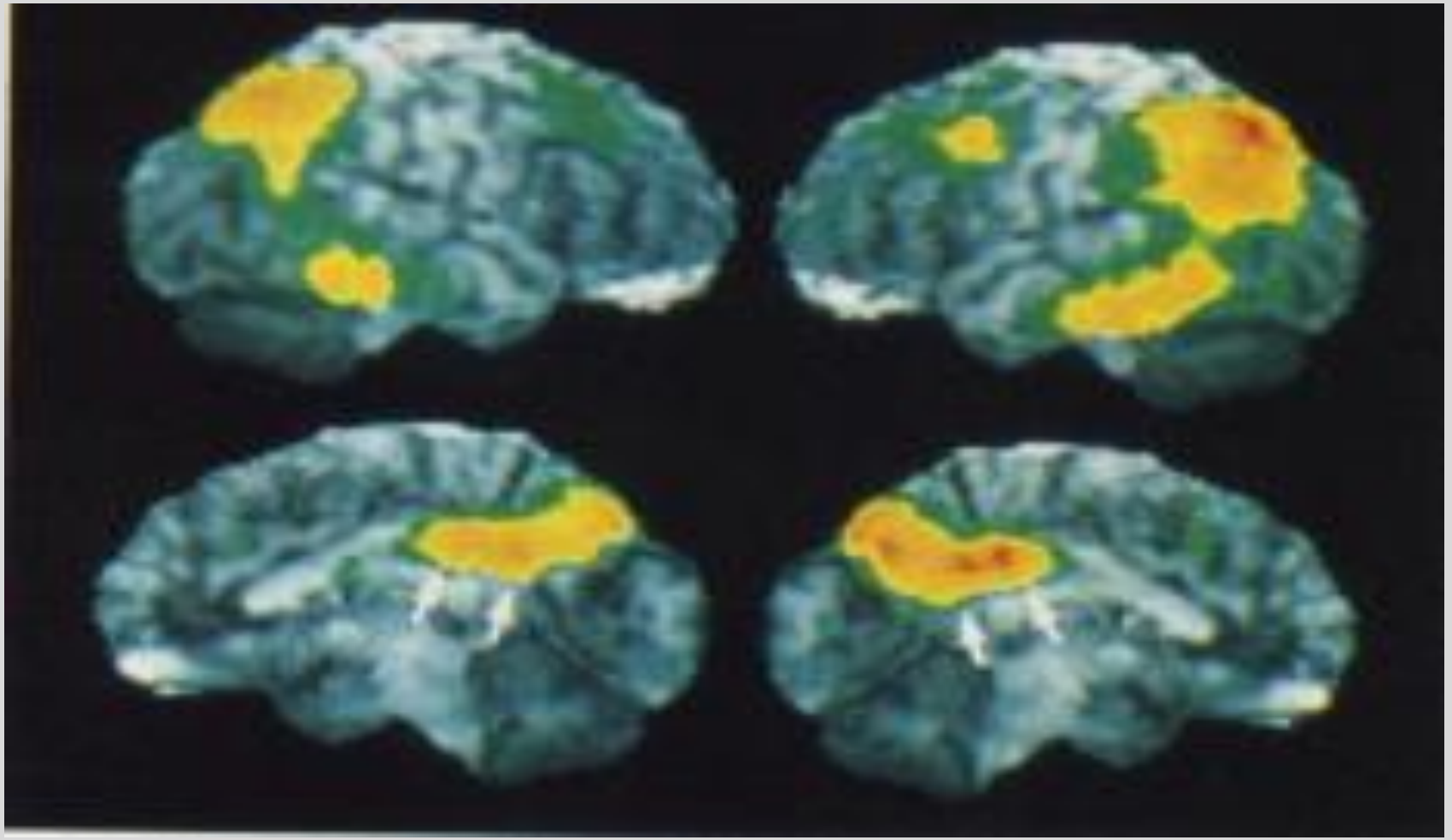

FDG-PET
Hypometabolism in
Posterior Cingulate Cortex

Minoshima et al, 1994

PCC and Episodic Memory Brain Network

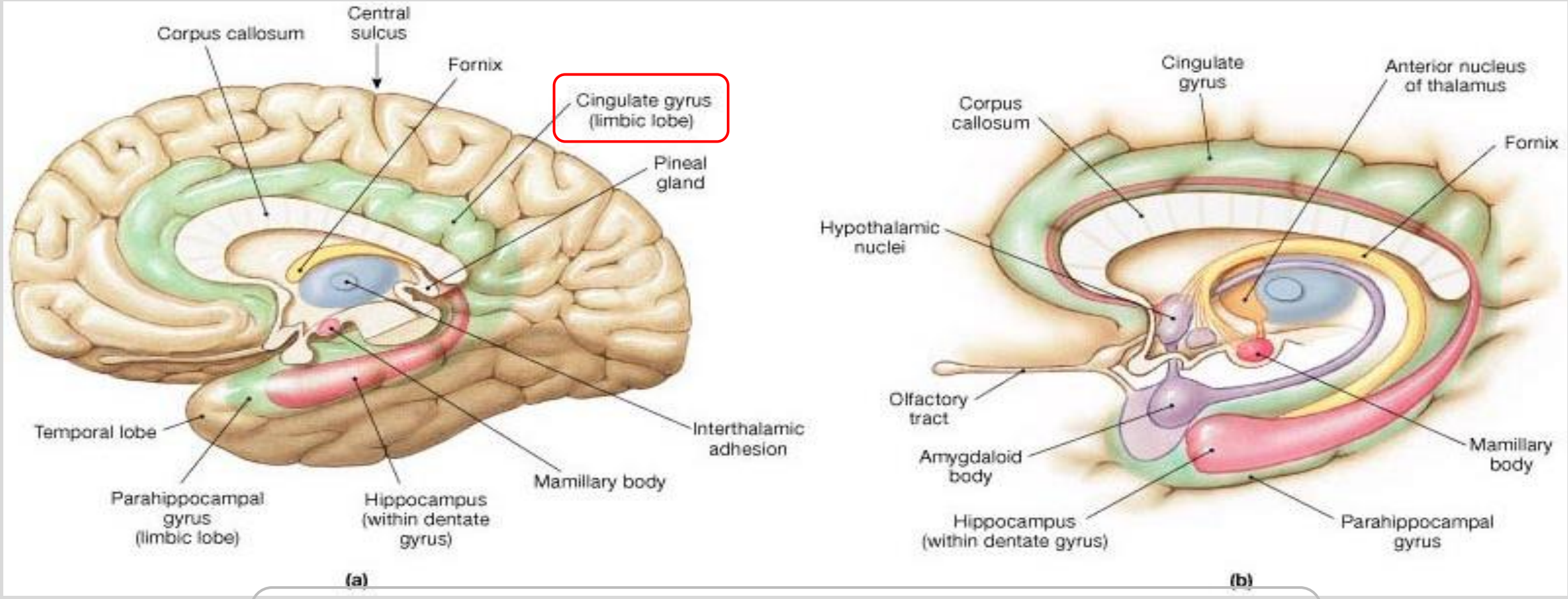

Papez circuit and episodic memory (memory for events, while remembering context and emotion)

Another PET discovery: The Default Mode Network

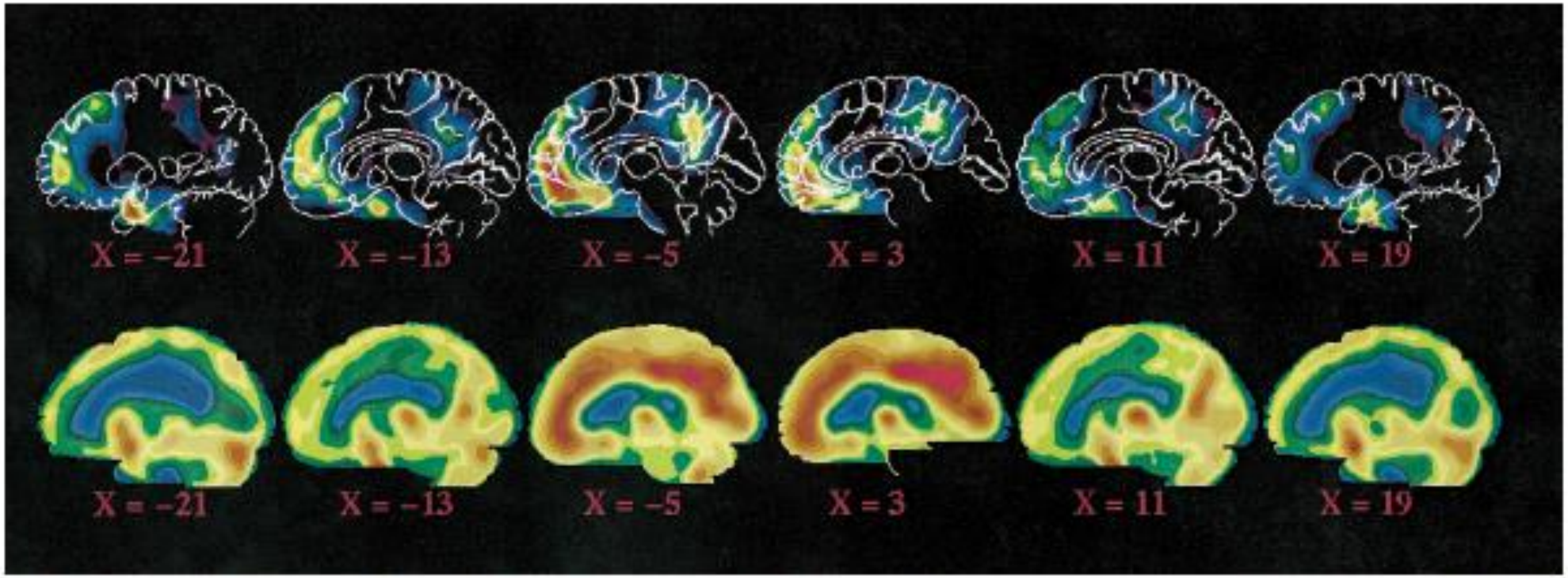

Fig. 5. Regions of the brain regularly observed to decrease their activity during attention-demanding cognitive tasks shown in sagittal projection (*Upper*) as compared with the blood flow of the brain while the subject rests quietly but is awake with eyes closed (*Lower*). The data in the top row are the same as those shown in Fig. 1, except in the sagittal projection, to emphasize the changes along the midline of the hemispheres. The data in the bottom row represent the blood flow of the brain and are the same data shown in horizontal projection in the top row of Fig. 2. The numbers below the images refer to the millimeters to the right (positive) or left (negative) of the midline.

Rest - Attention

CBF

Raichle, 2001

CBF, CMRO2, CMRGlu in AD

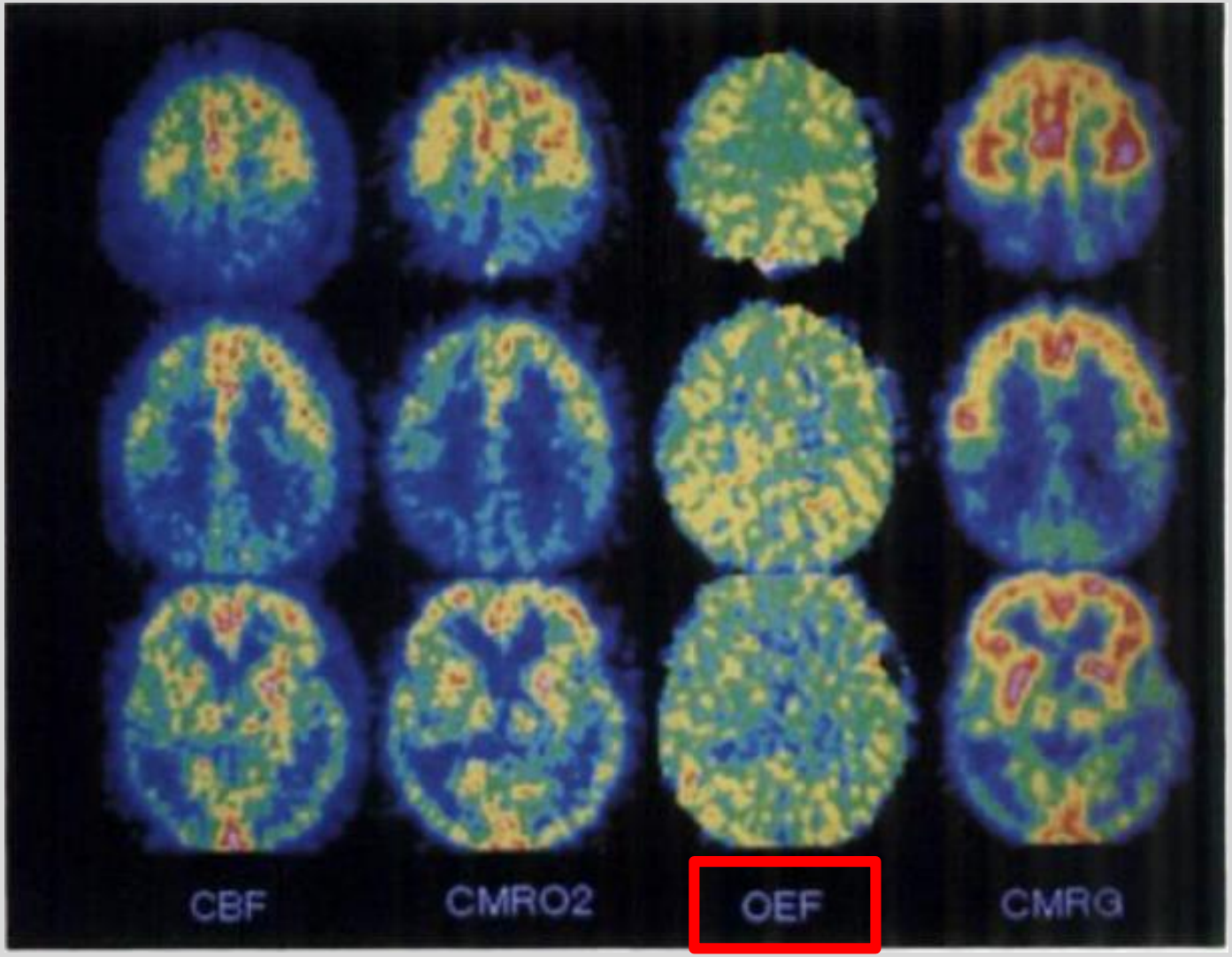

(1) There is no ischemia in AD

(2) CMRO2 versus CMRGlu

Fukuyama, 1994

Oxygen to Glucose Metabolic Index

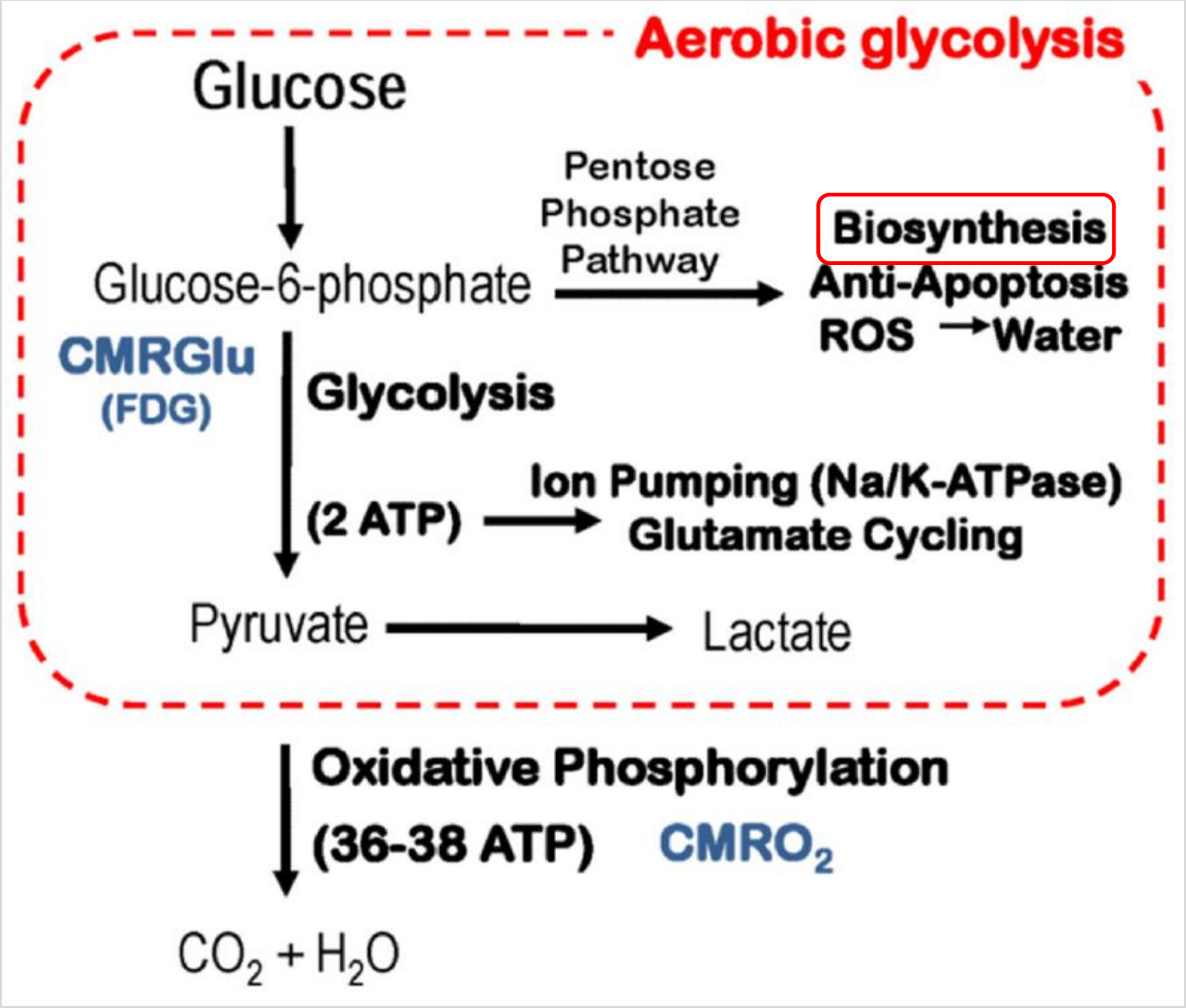

Oxygen to Glucose Metabolic Index

Early studies reported that the whole-brain average oxygen-to-glucose index was around 5.5.

If glucose is entirely consumed via oxidative pathways, the index should be 6, as 6 moles of oxygen are required to oxidize 1 mole of glucose. An index of 5.5 indicates that nearly 10% of the brain's glucose consumption at rest does not undergo oxidative phosphorylation.

The lowest rates aerobic glycolysis were found in the cerebellum and medial temporal lobe, whereas the highest were found in the prefrontal and parietal cortices

The expression of genes related to synaptic plasticity and development is enriched in brain regions with high levels of aerobic glycolysis. This suggests that a portion of the brain's non-oxidative glucose metabolism in spent on synaptic plasticity and other biosynthetic processes

Oxygen to Glucose Metabolic Index

Some researches strongly suggest that physiological synaptic activity associated with aerobic glycolysis regulates interstitial fluid Aβ levels and Aβ plaque formation.

The highest rates of aerobic glycolysis were found in the prefrontal and parietal cortices (Default Mode Network / DMN)

Data suggest that high rates of aerobic glycolysis may put a brain region at risk for developing amyloid plaques later in life

Oxygen to Glucose Metabolic Index

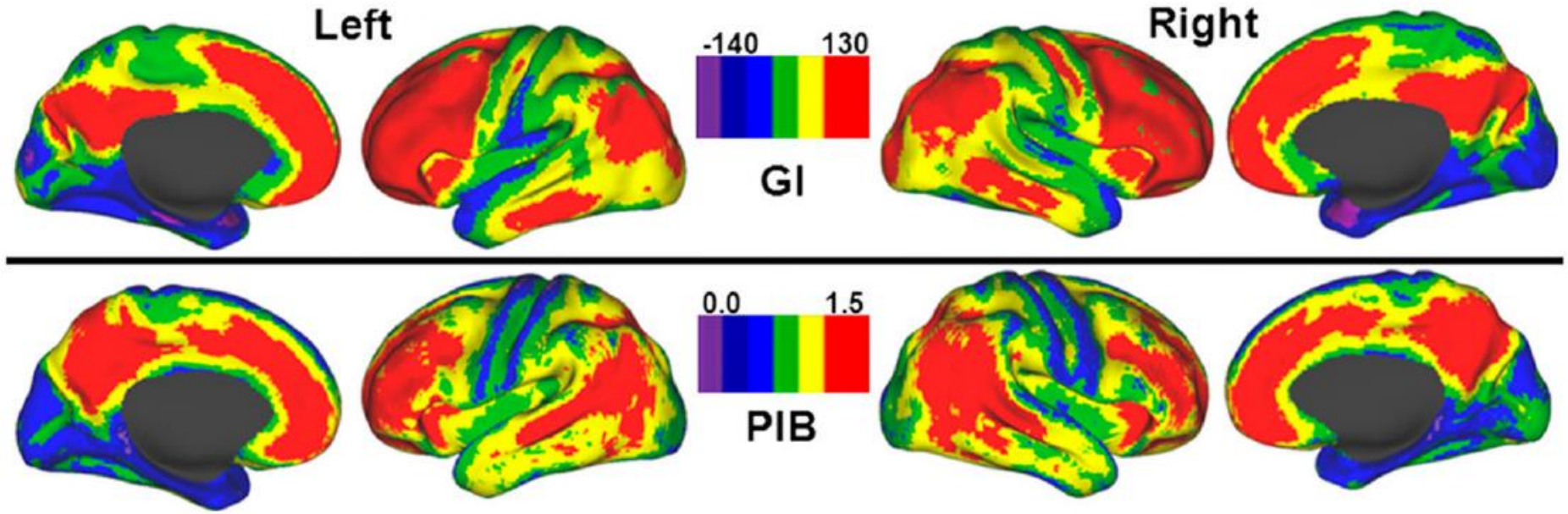

Figure 7.
Maps showing lateral and medial cortical surfaces of the human brain on which are depicted the mean distribution of AG in units of the GI in 33 neurologically normal young adults and ^{11}C-PIB binding potentials in 11 individuals with DAT. Reproduced with permission from Vlassenko et al. [20].

Aerobic Glycolytic Index
in young controls

Amyloid-PET
in AD

Vlassenko &
Raichle, 2015

Oxygen to Glucose Metabolic Index

Some researches strongly suggest that physiological synaptic activity associated with aerobic glycolysis regulates interstitial fluid Aβ levels and Aβ plaque formation.

The highest rates of aerobic glycolysis were found in the prefrontal and parietal cortices

(Default Mode Network / DMN)

Data suggest that high rates of aerobic glycolysis may put a brain region at risk for developing amyloid plaques later in life

CMRglc has been shown to decrease to a greater extent than CMRO2 in individuals with AD.

This indicates that aerobic glycolysis decreases in AD (at least in early stages)

Atrophy and molecular imaging

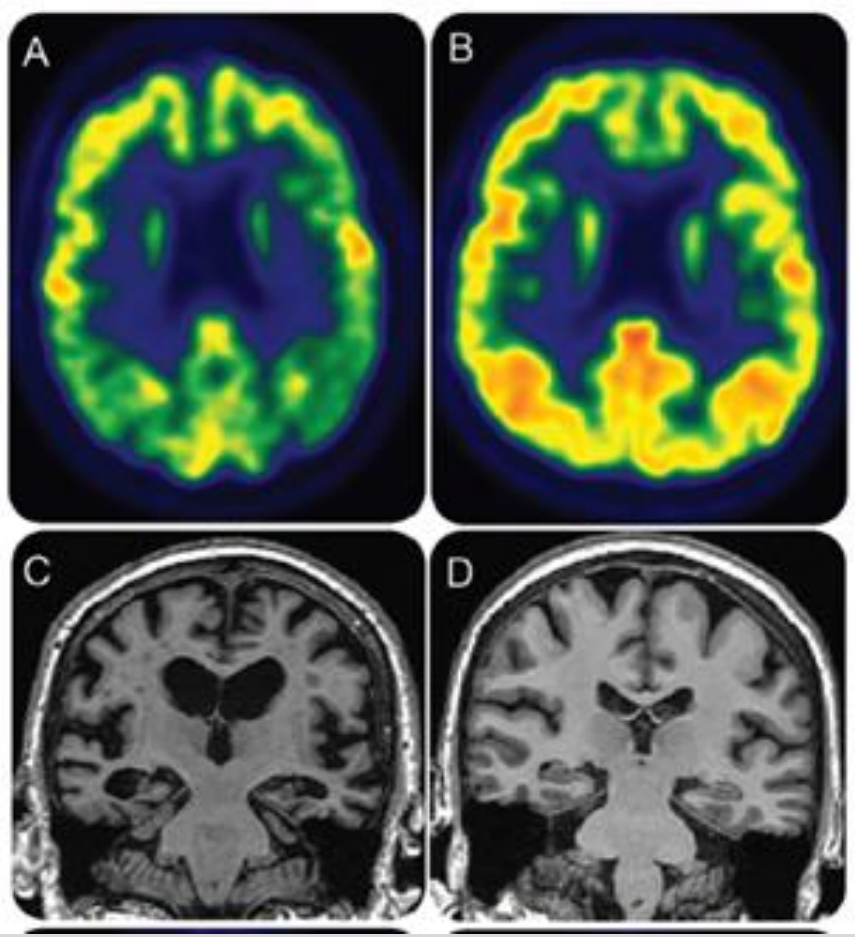

Regional glucose metabolic abnormalities are not the result of atrophy in Alzheimer's disease

Ibanez et al, 1998

Correction of metabolic values for atrophy

A biological model of AD: amyloid & tau

- Hypothetical model of dynamic evolution of brain biomarkers in AD

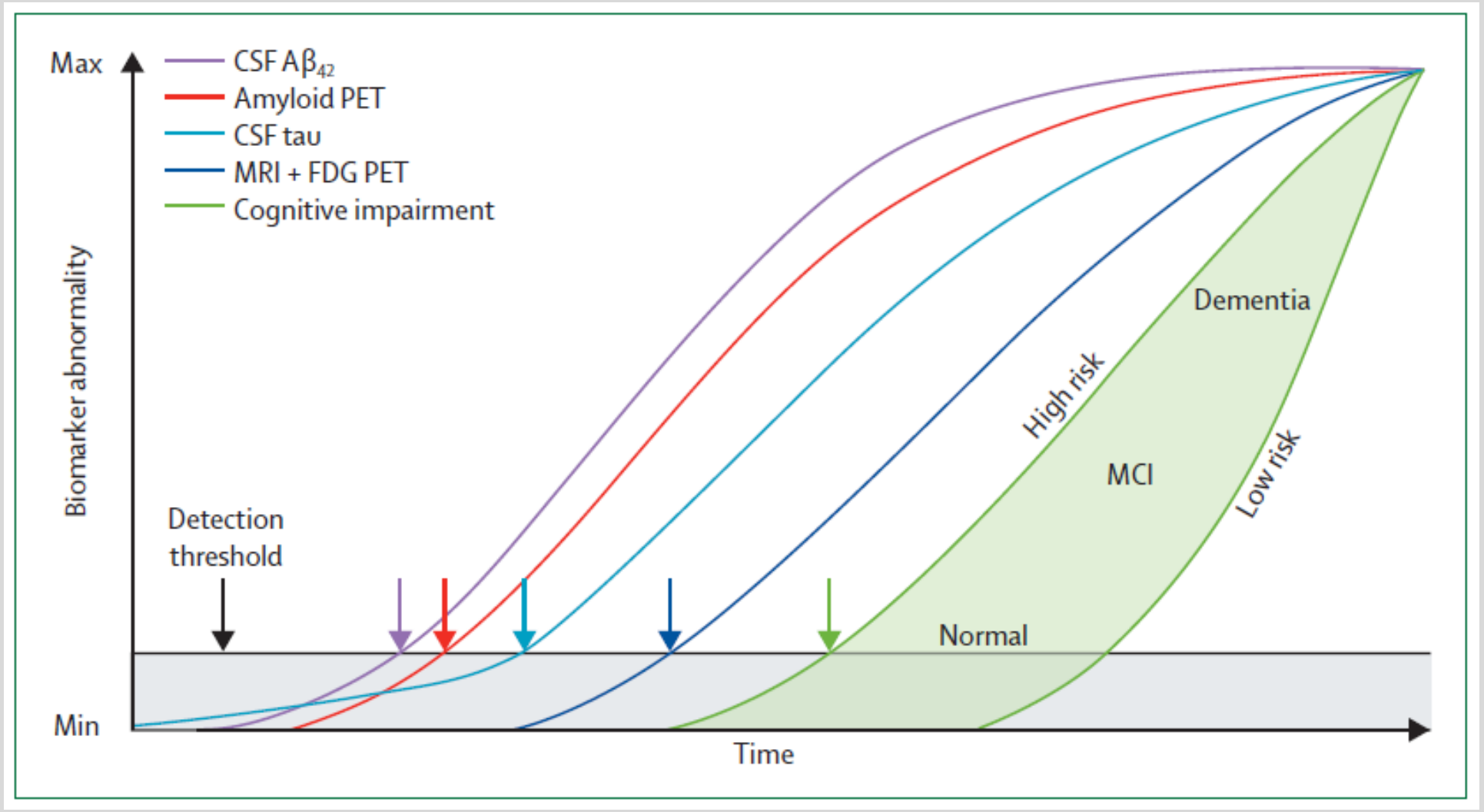

A biological model of AD: amyloid & glucose metabolism in transgenic (McGill R Thy1 APP) rat

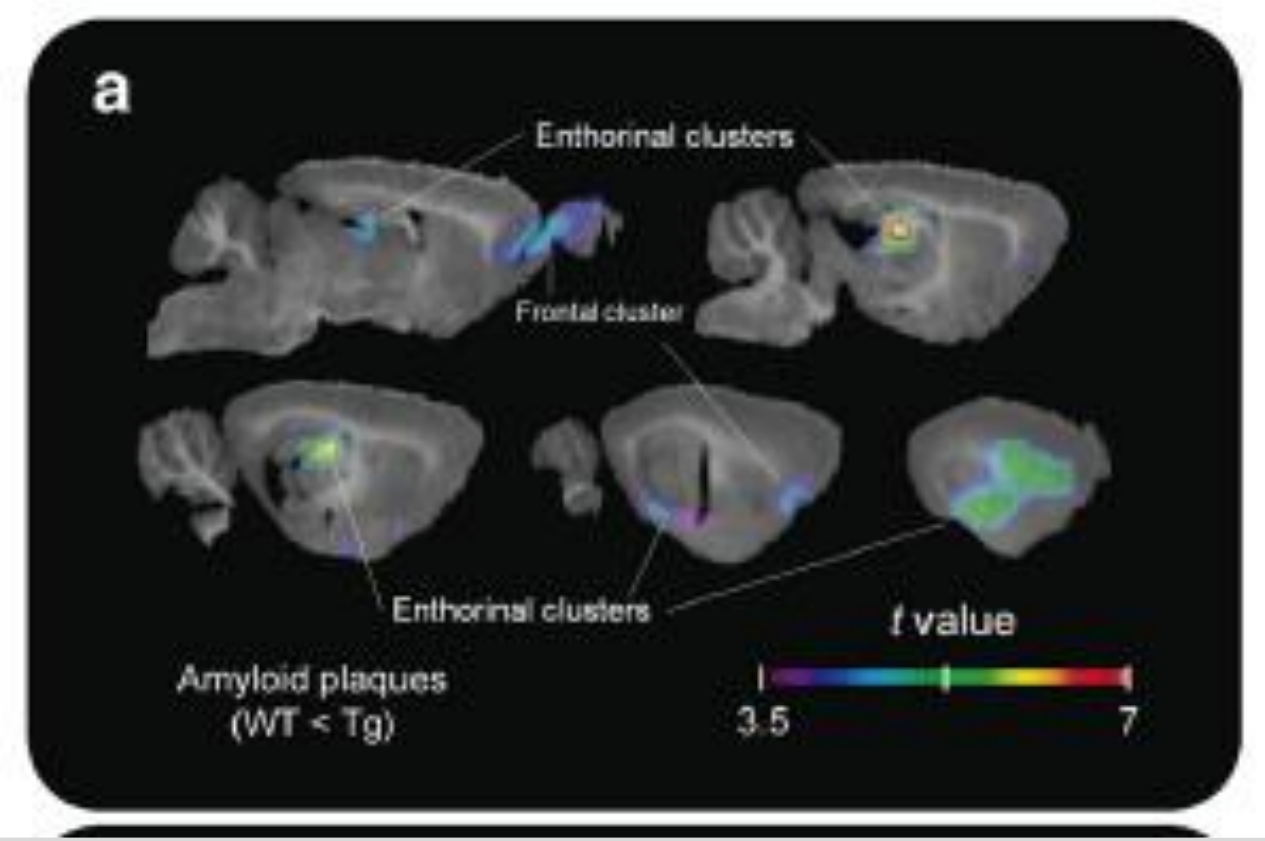

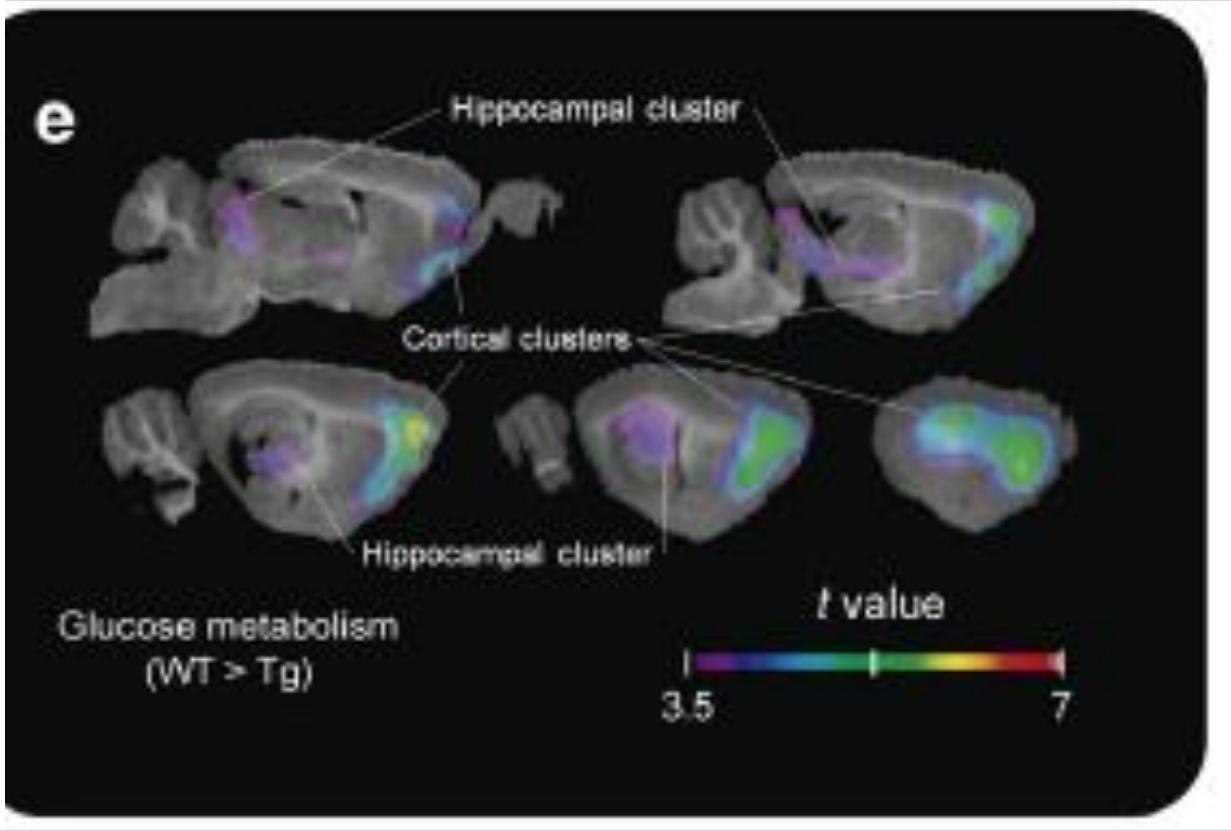

PET-amyloid

PET-FDG

Preclinical stages of AD (Sperling, 2011)

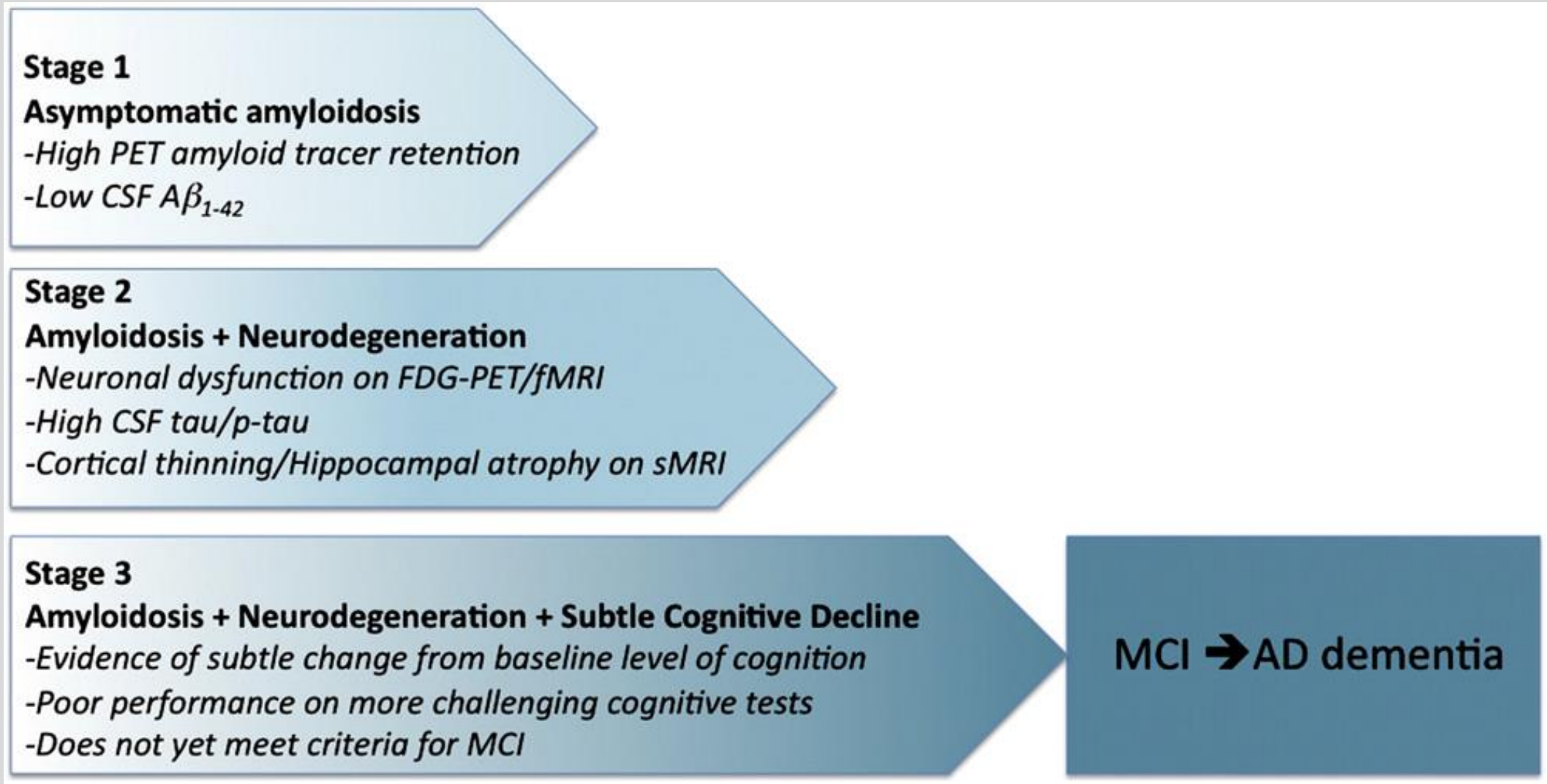

FDG-PET in asymptomatic participant

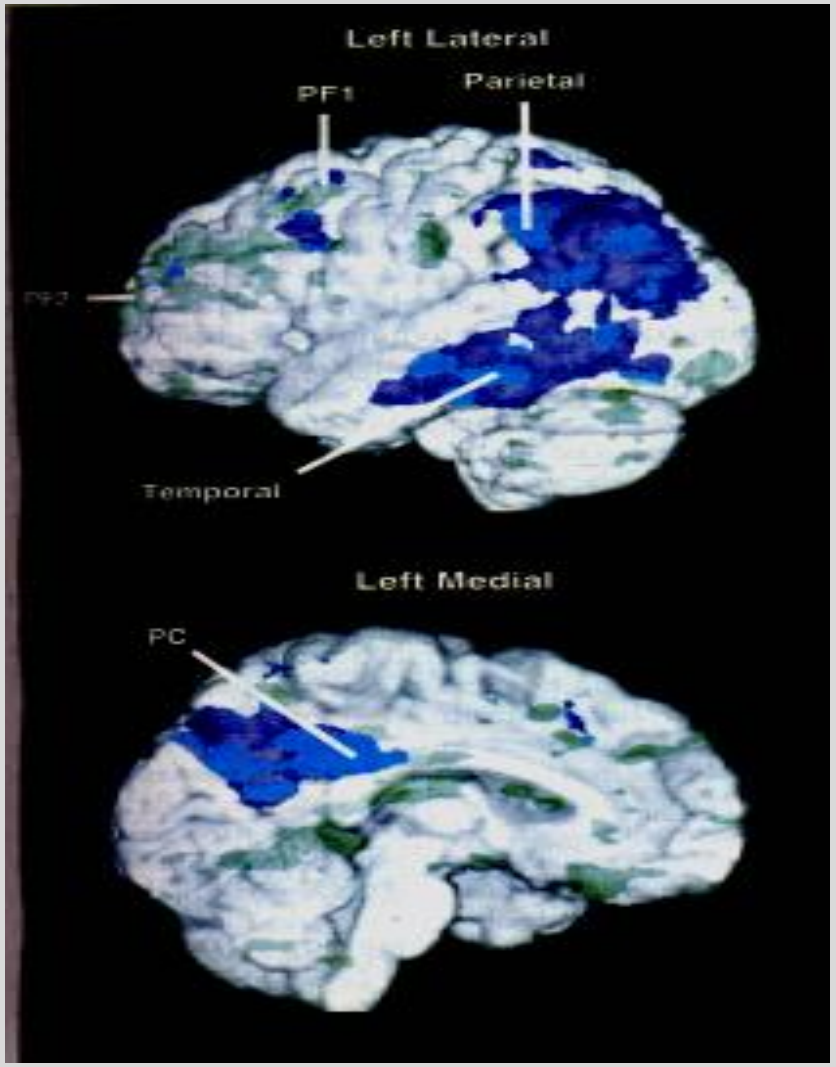

Characteristic metabolic pattern
in subjects at risk for AD:

family history and
e4 homozygotes

E.M. Reiman et al, 1996

Pittsburg compound-B (PiB) for amyloid-PET

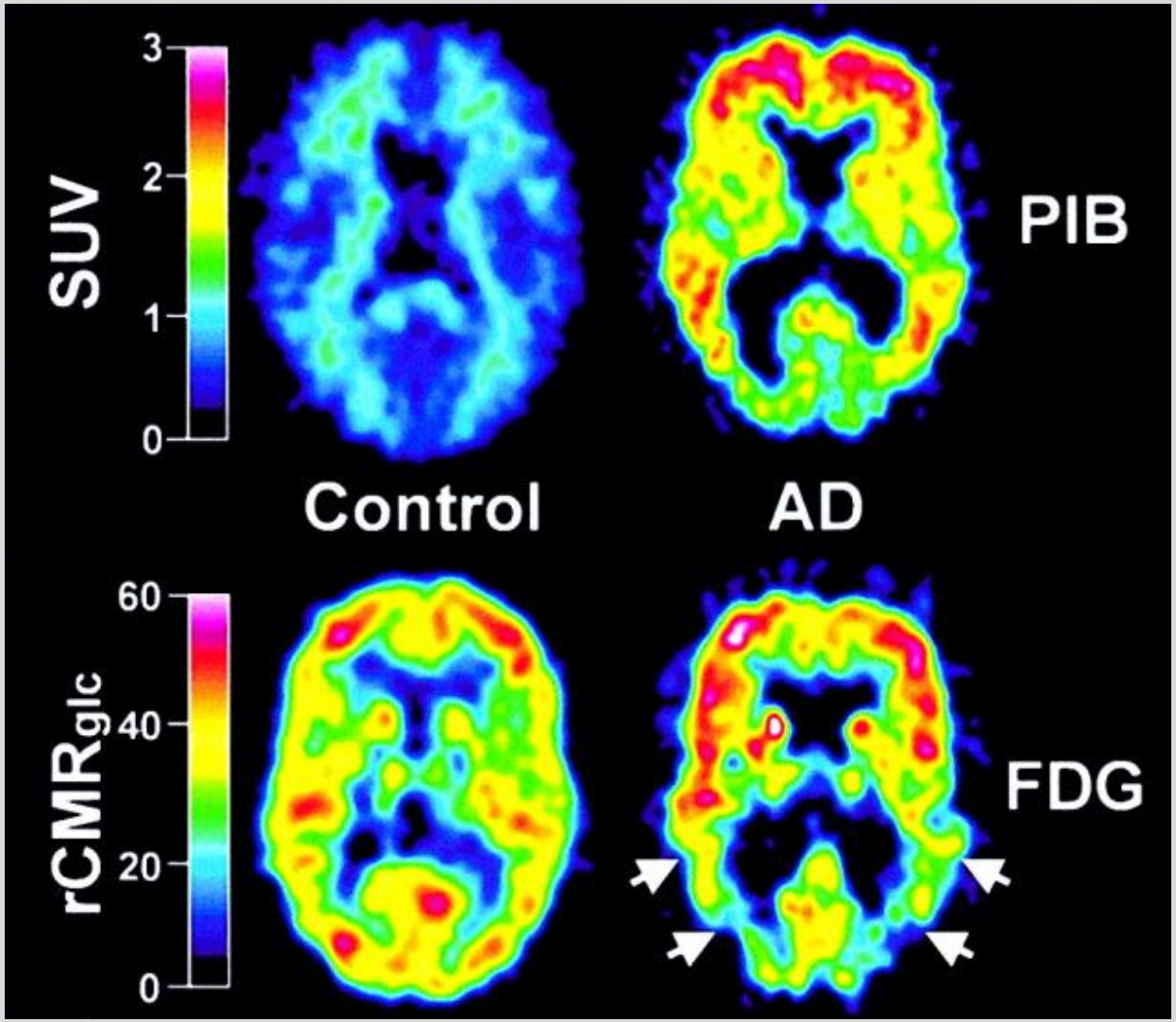

PiB is binding to β-pleated sheets

Klunk et al, 2004

Pittsburg compound-B (PiB) for amyloid-PET

Correlation between
in vivo PiB-PET
and post-mortem 6-CN-PiB

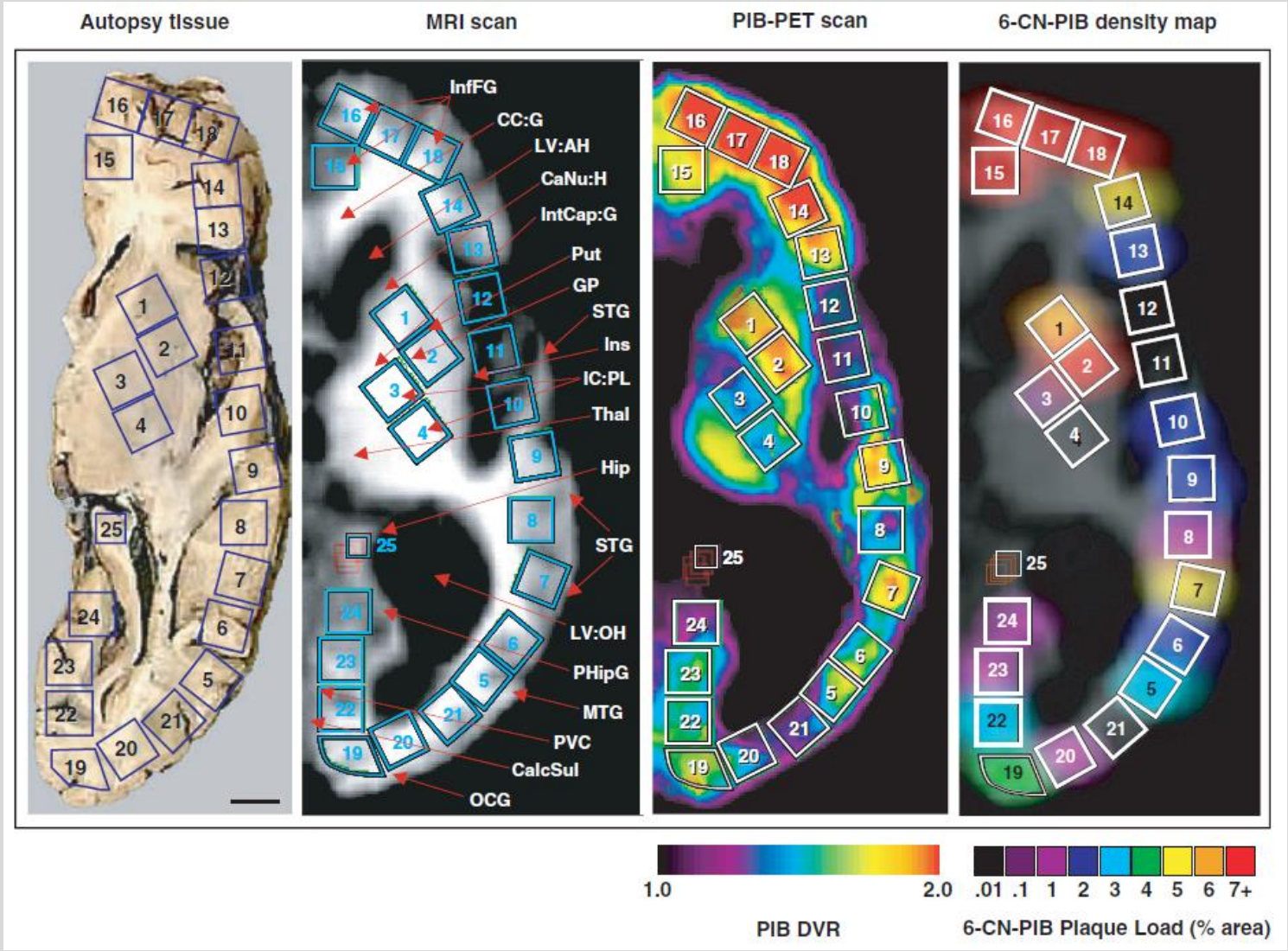

Ikonomovic et al, Brain 2008

PET-amyloid & amyloid stages in AD

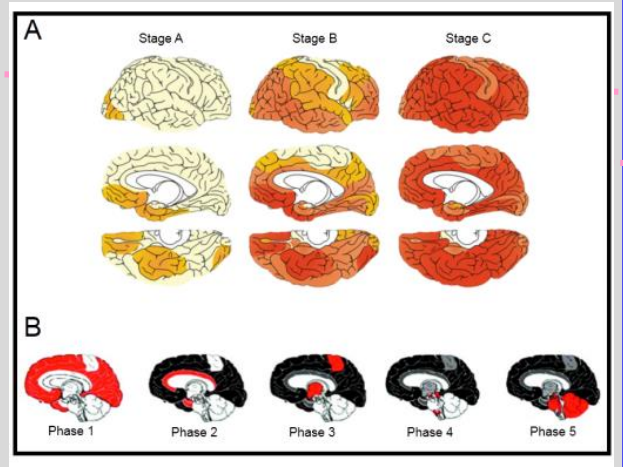

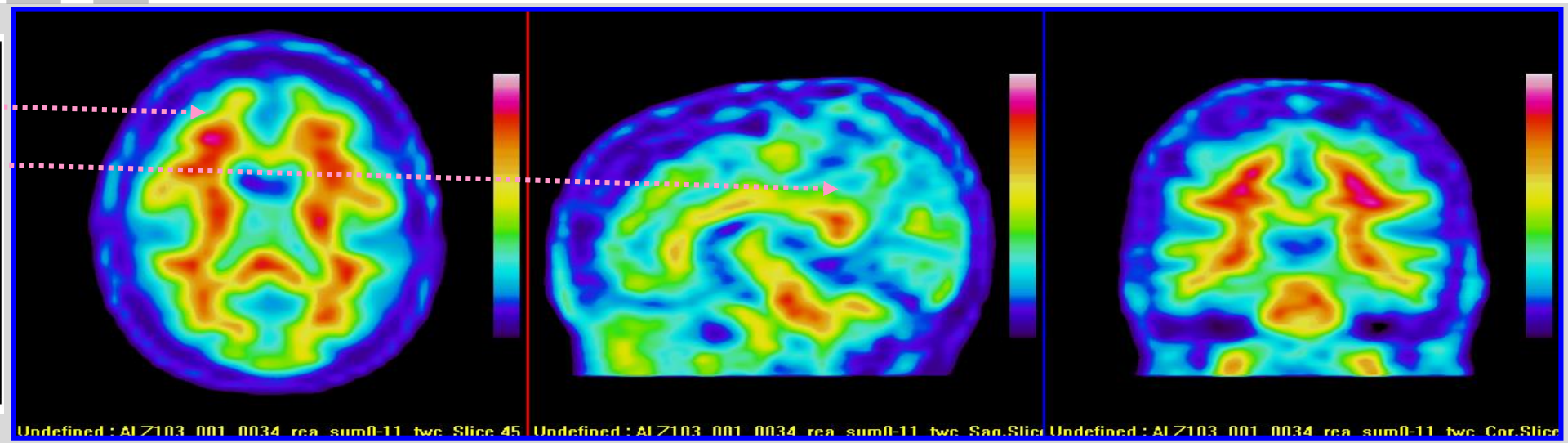

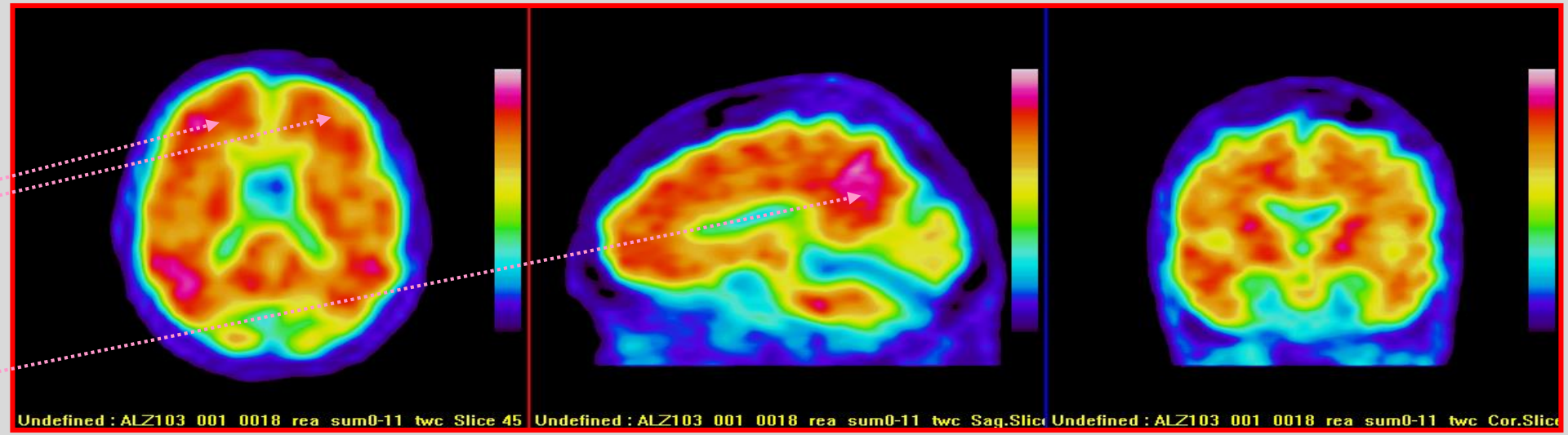

Frontal

PCC

Post mortem NFT/tau brain lesions in AD

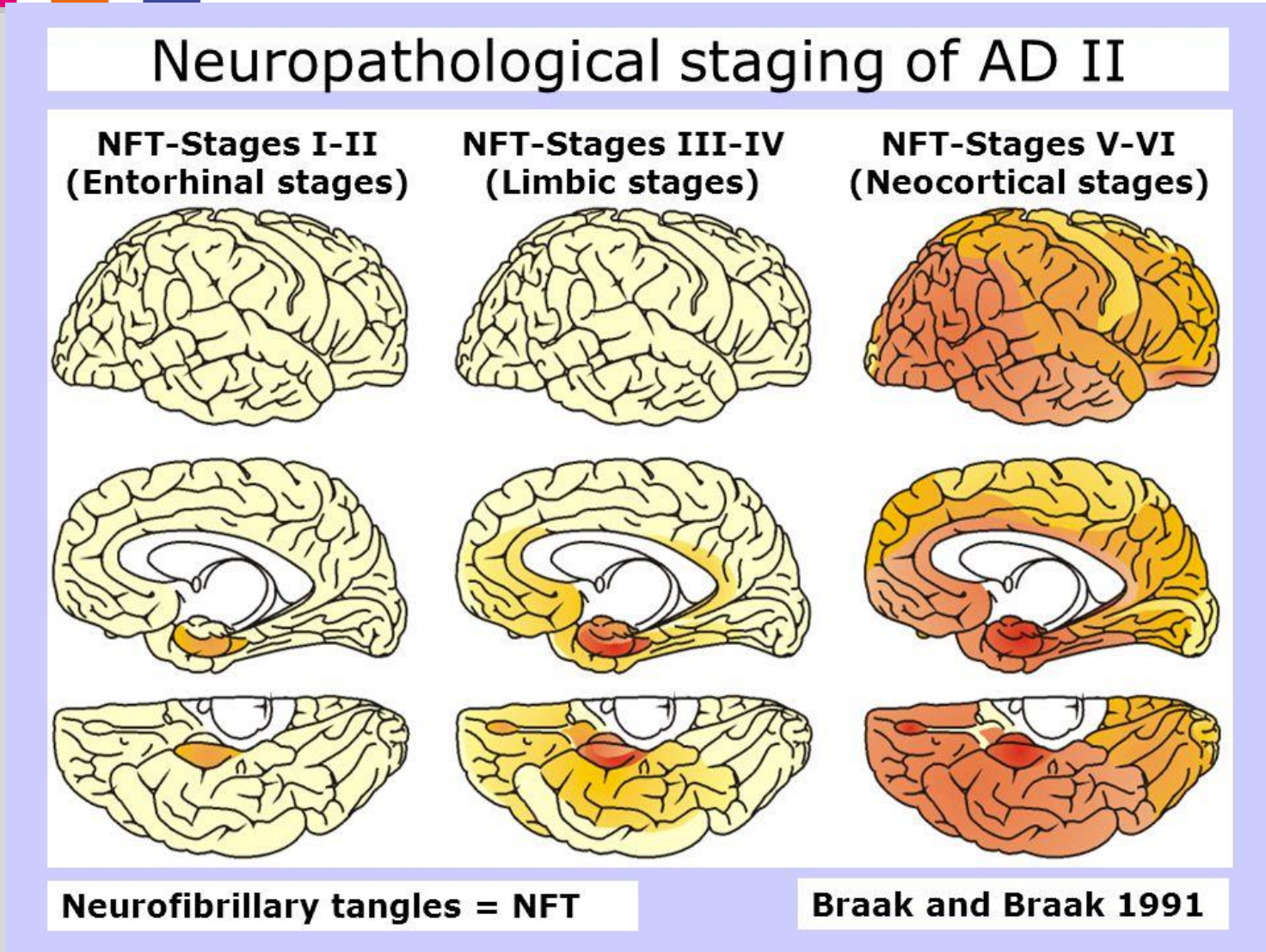

tau-PET tracer [18F]THK5351

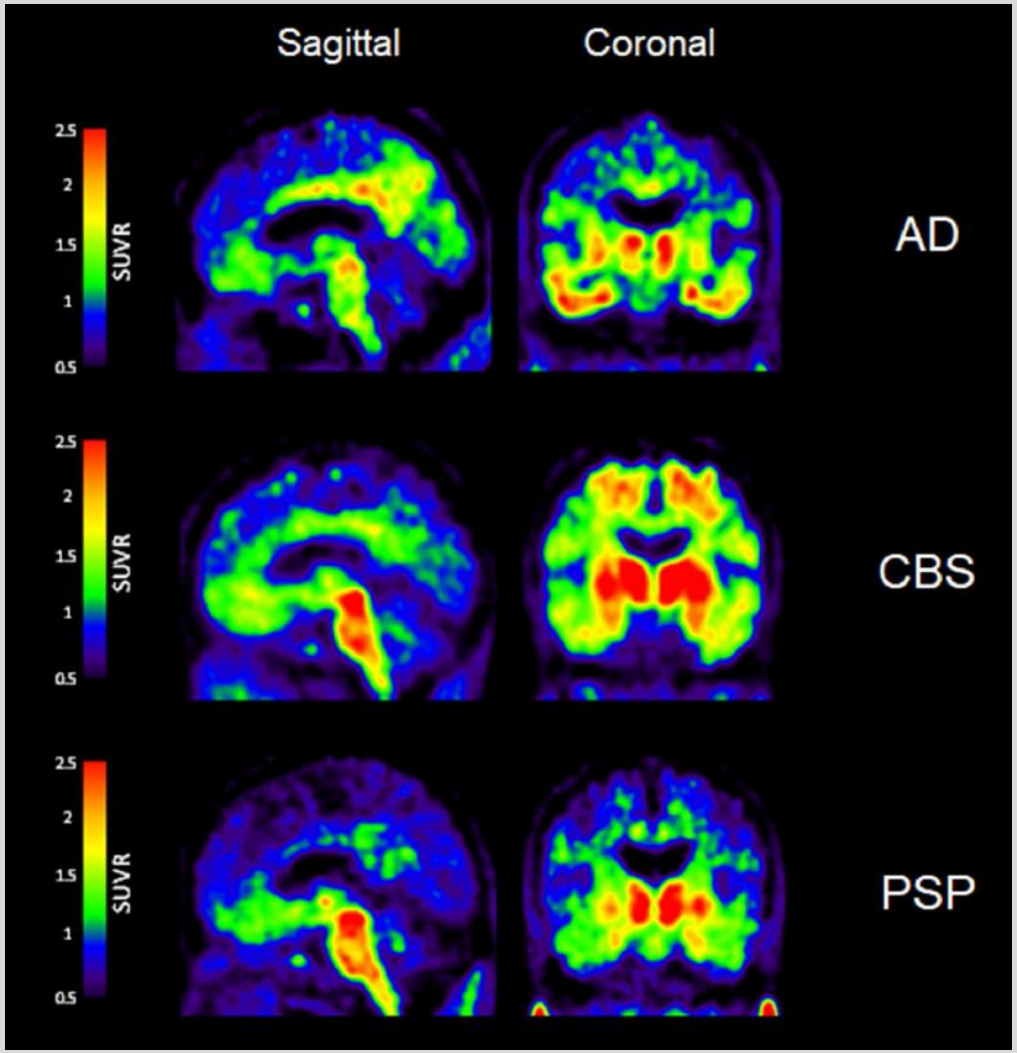

β-sheet-binding compound;

Higher affinity for tau fibrils than for Aβ fibrils

Amyloid +?

Okamura, 2018

Distribution of tau-PET tracer versus PiB

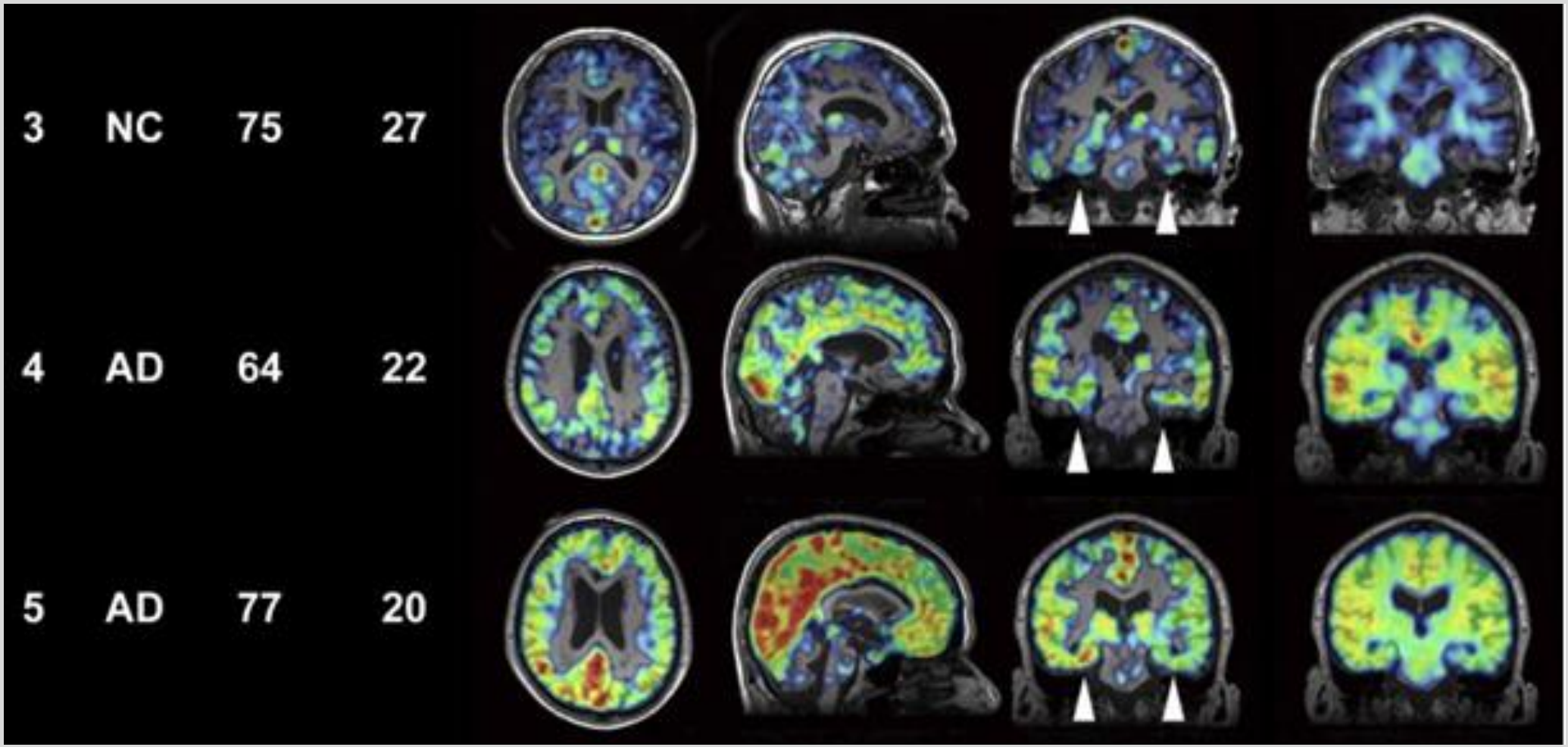

Neuroinflammation in AD

Neuroinflammation in the form of microglial and astrocyte activation has been recognised to be a component of AD pathological cascade.

Microglia may express a reparative phenotype, acting to clear cellular debris and remodel synapses or, alternatively, a cidal phenotype releasing cytokines which damage neurons (M2/M1 paradigm). It remains unresolved which phenotype is preferentially expressed at different time points along the AD trajectory.

Translocator Protein (TSPO) is expressed on microglia and positron emission tomography (PET) studies in humans have shown higher signals in prodromal Alzheimer's disease which could support an initially protective role of microglia

Inter-subject variability in binding affinity exists due to polymorphism in the TSPO gene

Neuroinflammation before tau in AD

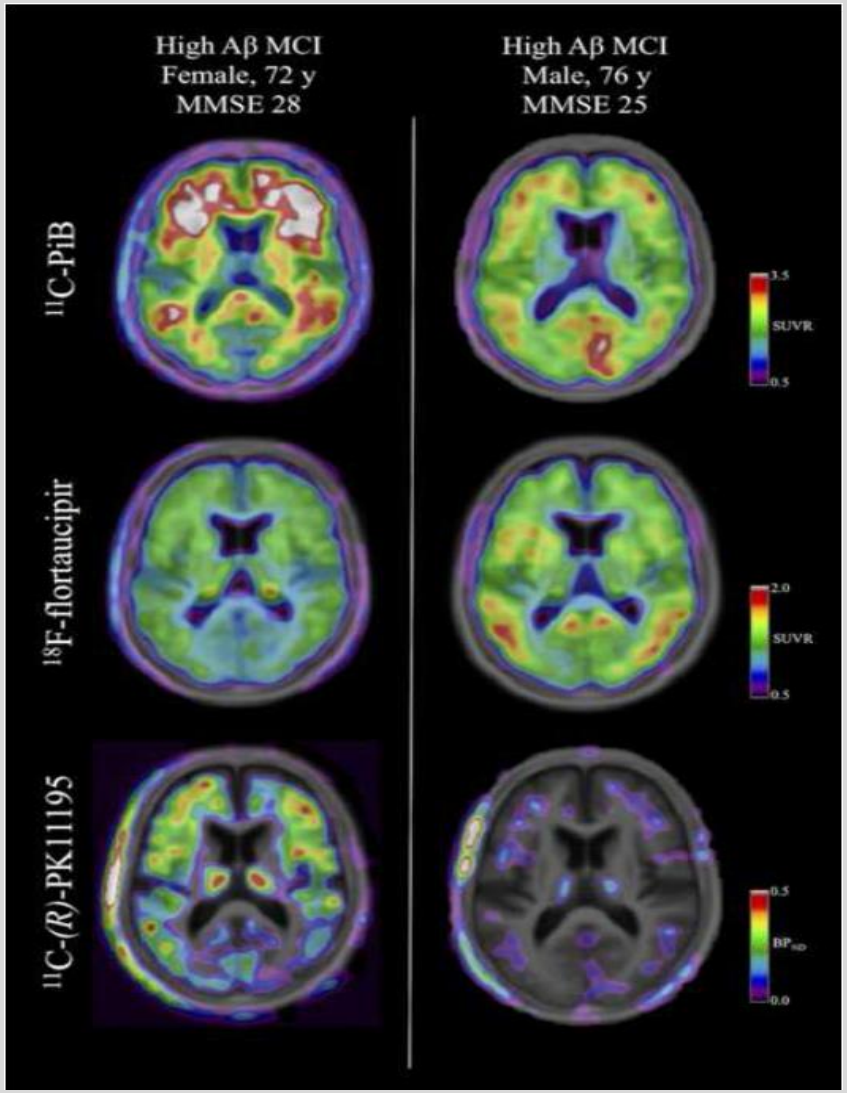

Amyloid

Tau

Inflammation (clearing amyloid?)

A biphasic course (reparative followed by cidal inflammation) was suggested in a longitudinal study

Ismael, 2020

Reactive astrocytes in (PiB+) MCI

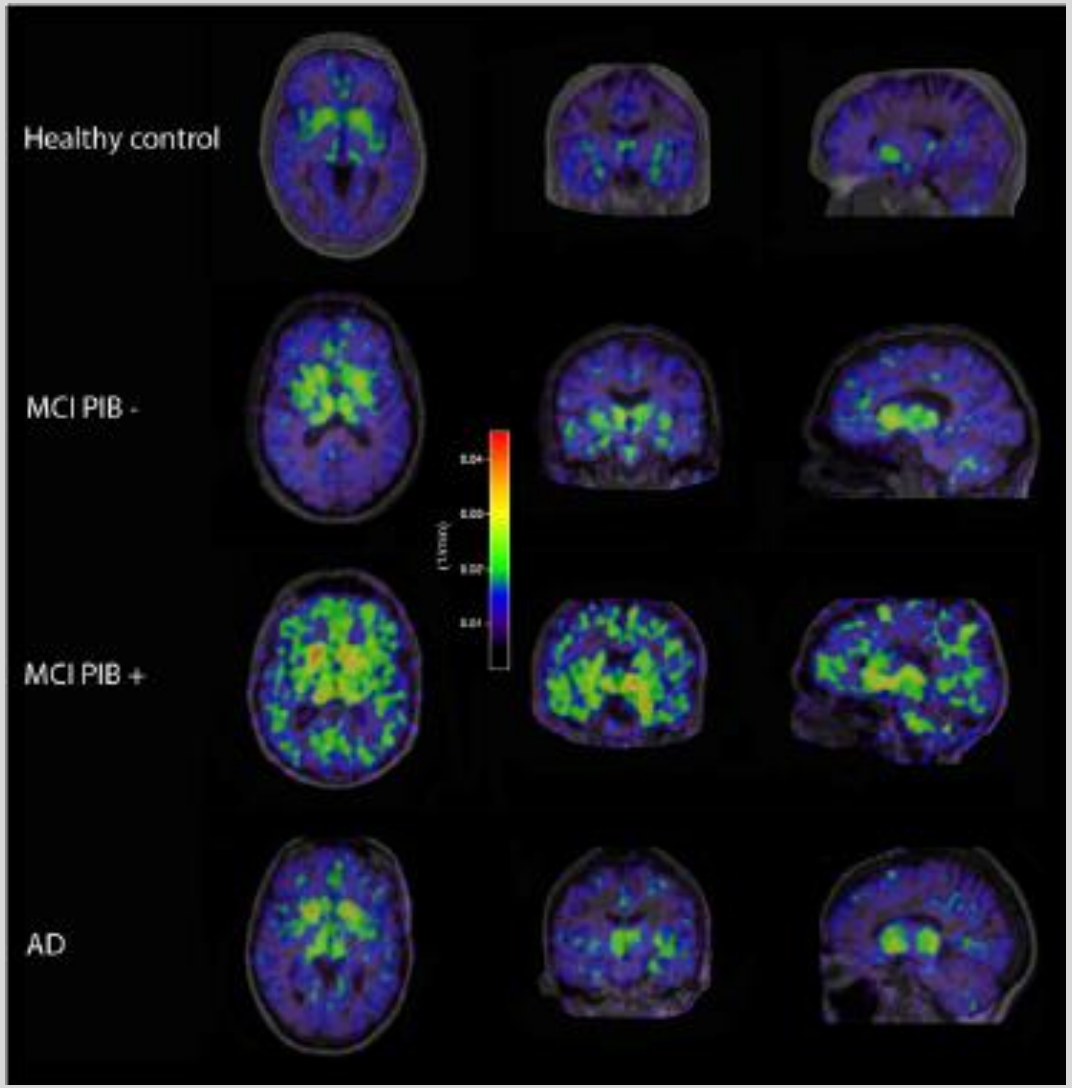

[11C]-deuterium L deprenyl

(binding to MAO-B)

Carter, 2012

[18F]THK5351 binds to tau & MAO-B

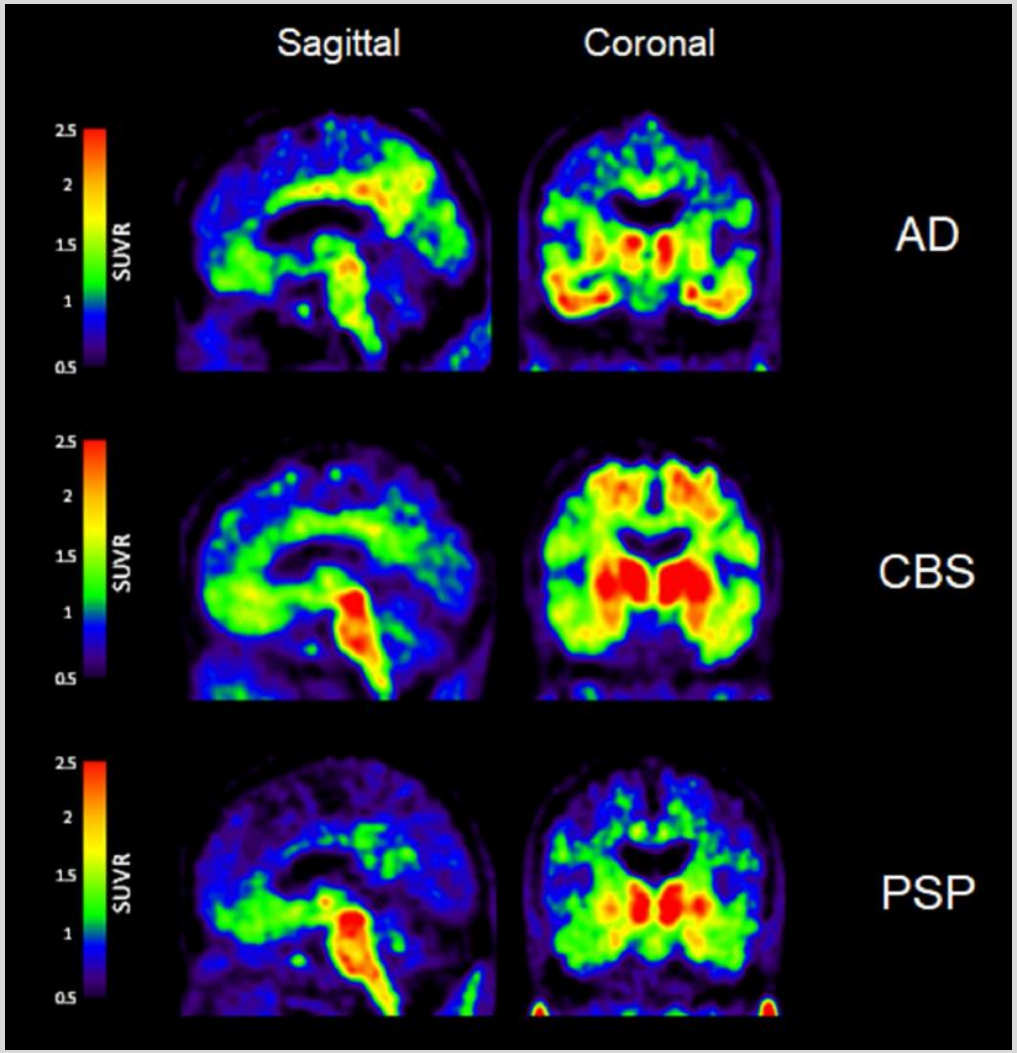

β-sheet-binding compound;

Higher affinity for tau fibrils than for Aβ fibrils

Amyloid +?

Okamura, 2018

Assessment of the cholinergic system

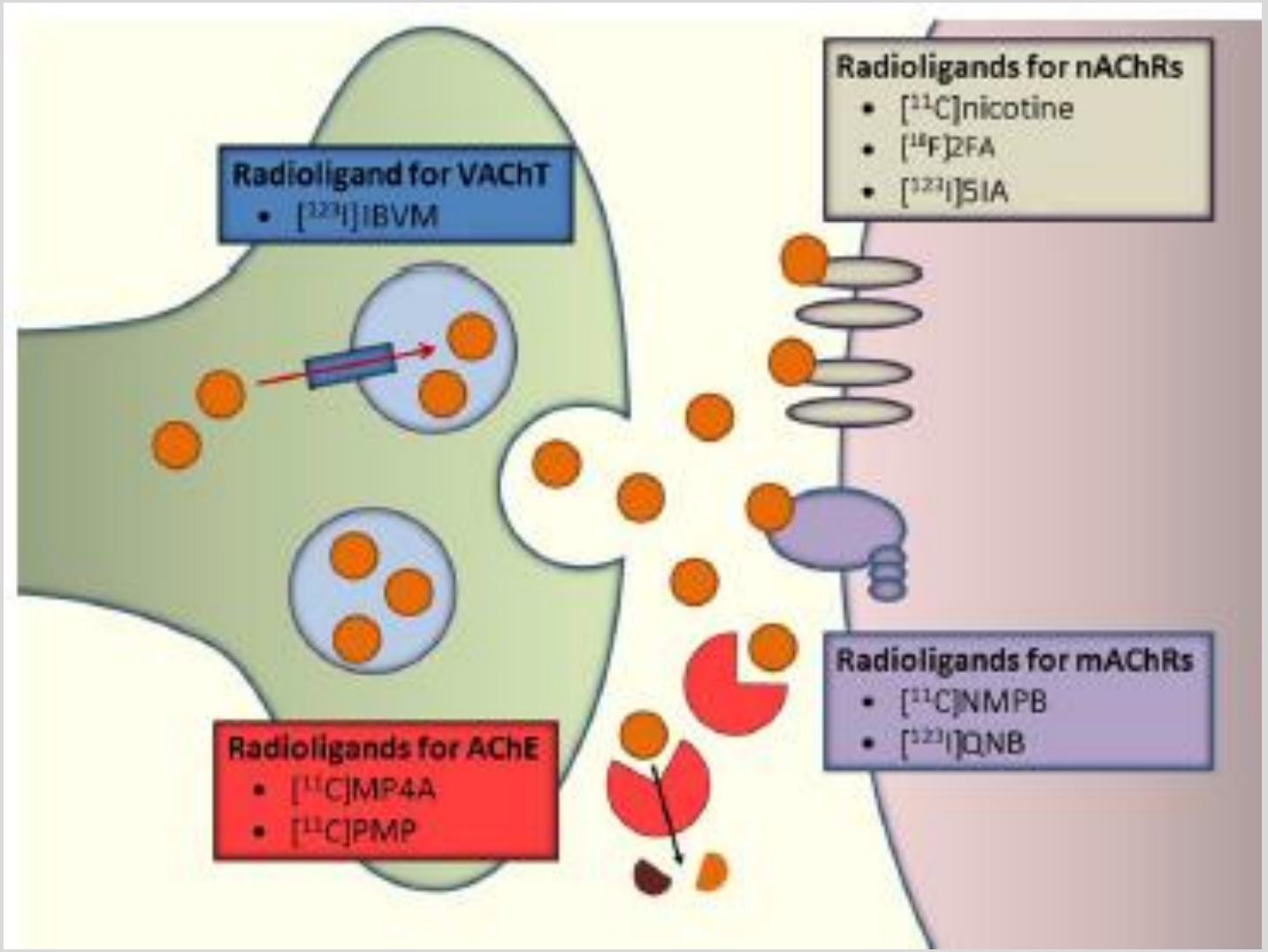

Assessment of the cholinergic system

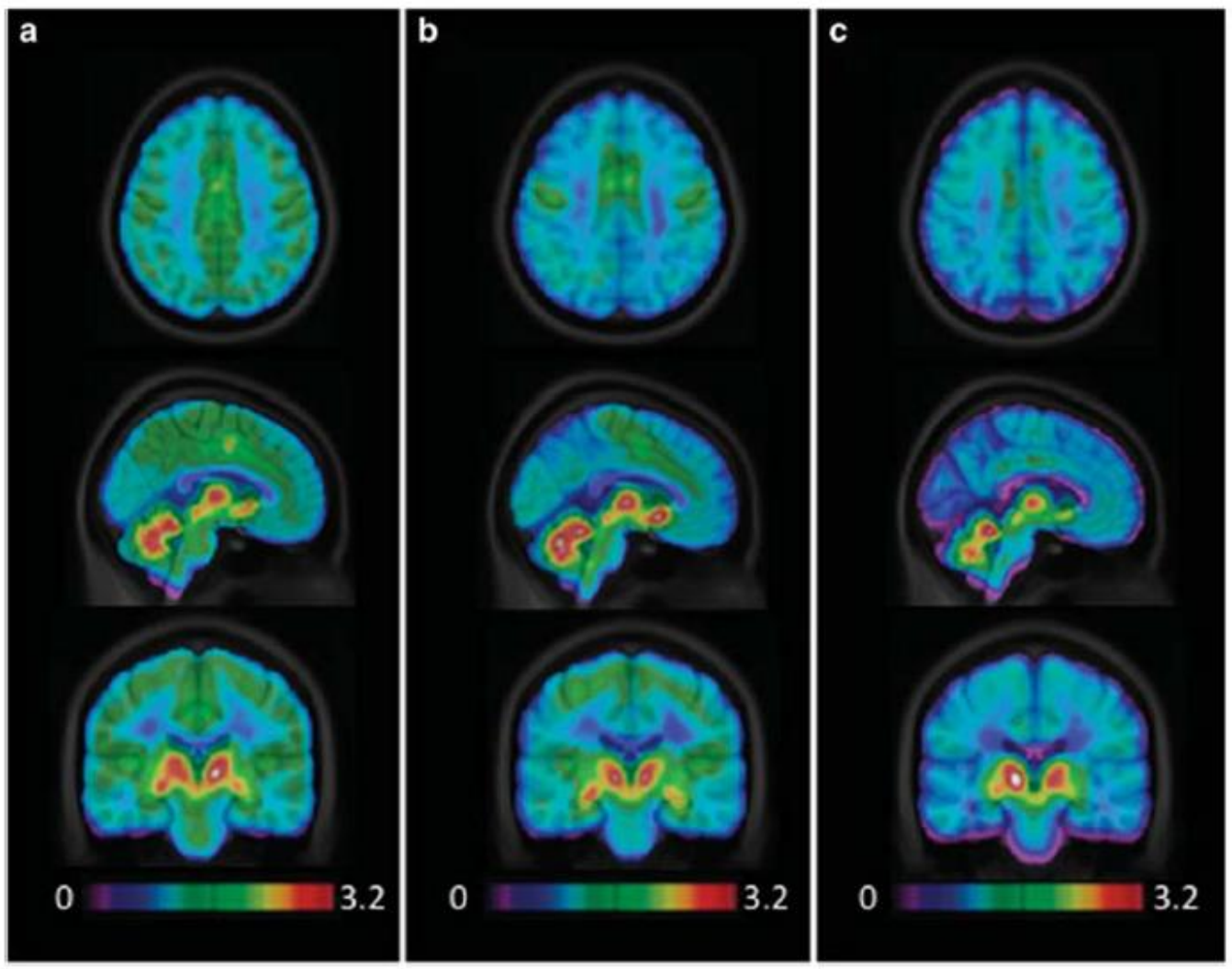

Decrease of cortical presynaptic Vesicular Acetylcholine transporter (VAChT) studied with [18F]FEOBV-PET in AD

The hippocampus, innervated by septal cholinergic neurons, would be less affected.

Aghourian, 2017

Assessment of the cholinergic system

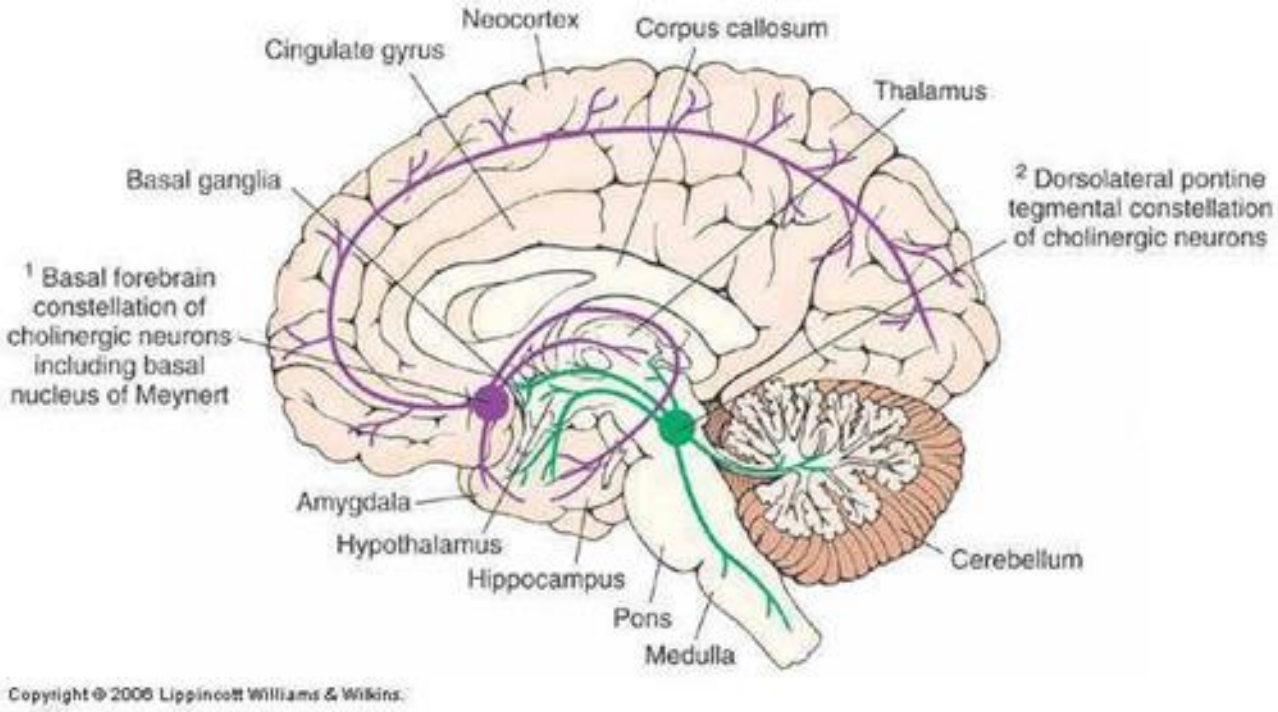

Neocortical and amygdaloid functional changes of the cholinergic system (using AchE radiotracer) are an early and leading event in AD, rather than the consequence of neurodegeneration of basal nuclei.

Herholz et al, 2004

Assessment of the cholinergic system

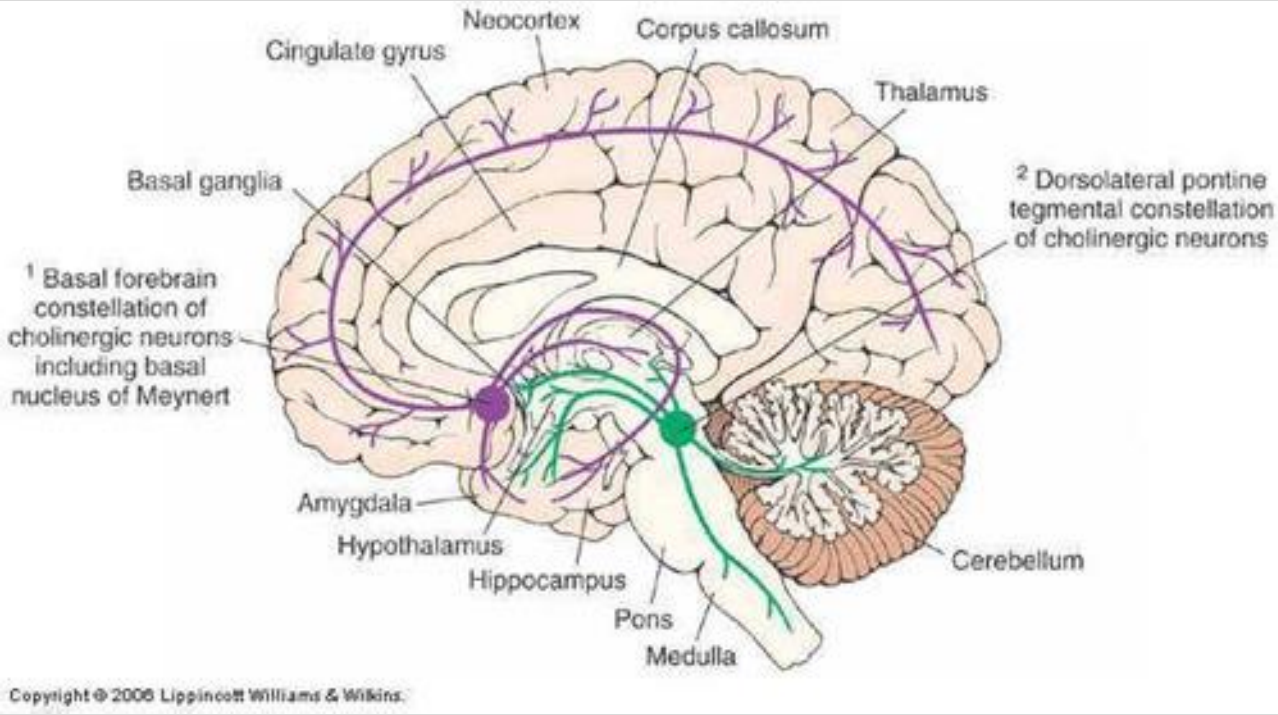

Basal forebrain volume reliably predicts the cortical spread of Alzheimer's degeneration.

Fernandez-Cabello, 2020

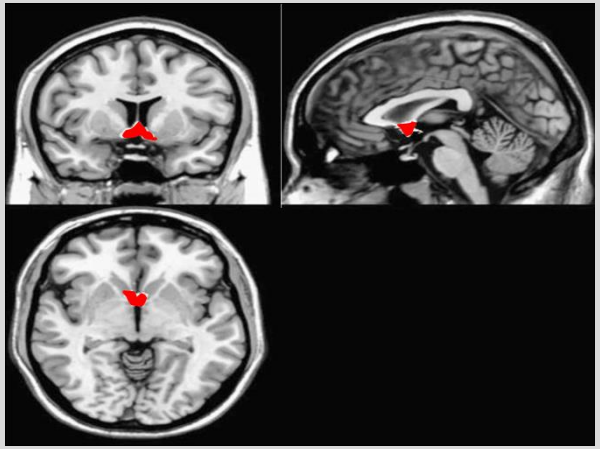

Assessment of the serotoninergic system

Midbrain Putamen Thalamus

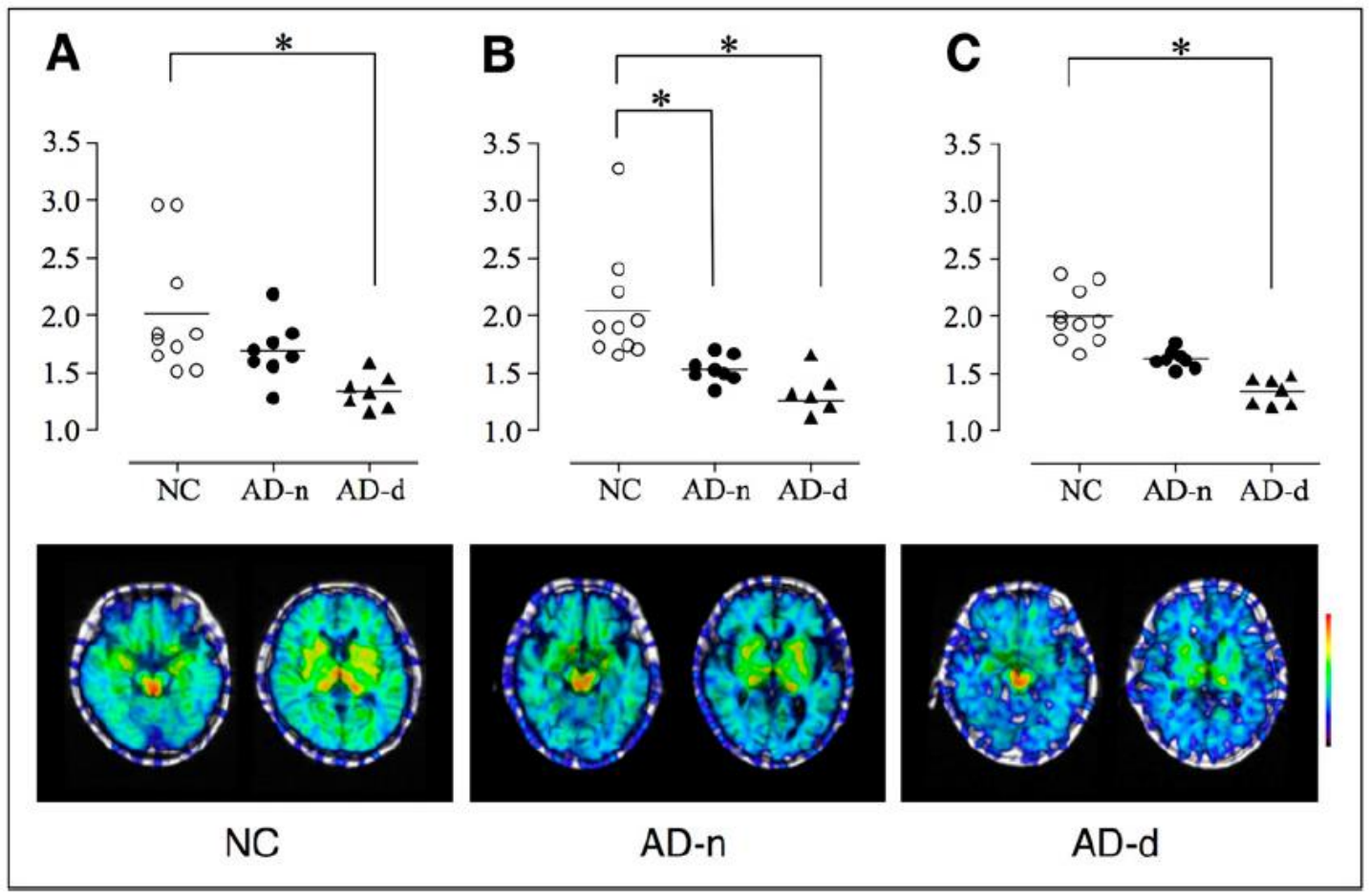

Assessment of

the Serotonin Reuptake Transporter (SERT)

with [11C]DASB-PET

in depressed & non depressed AD patients

Brain mGluR5 in AbPP transgenic mice (tg-ArcSwe) with amyloid beta pathology studied with in vivo [11C]ABP688 PET imaging

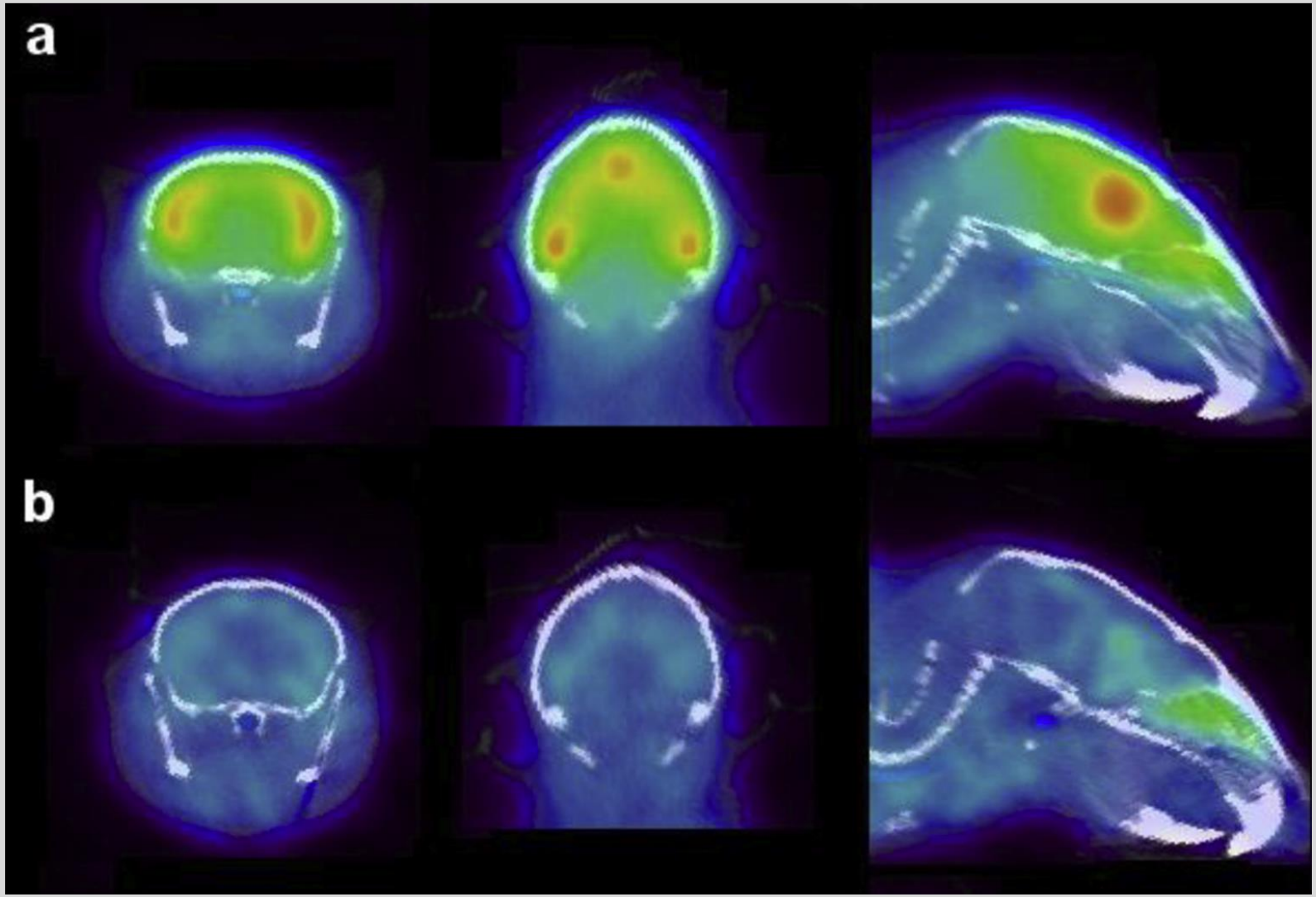

mGluR5 levels were found to decrease with age and tended to be higher in

tg-ArcSwe compared with wt mice

Saturation with cold substance

Glutamatergic pathway in AD

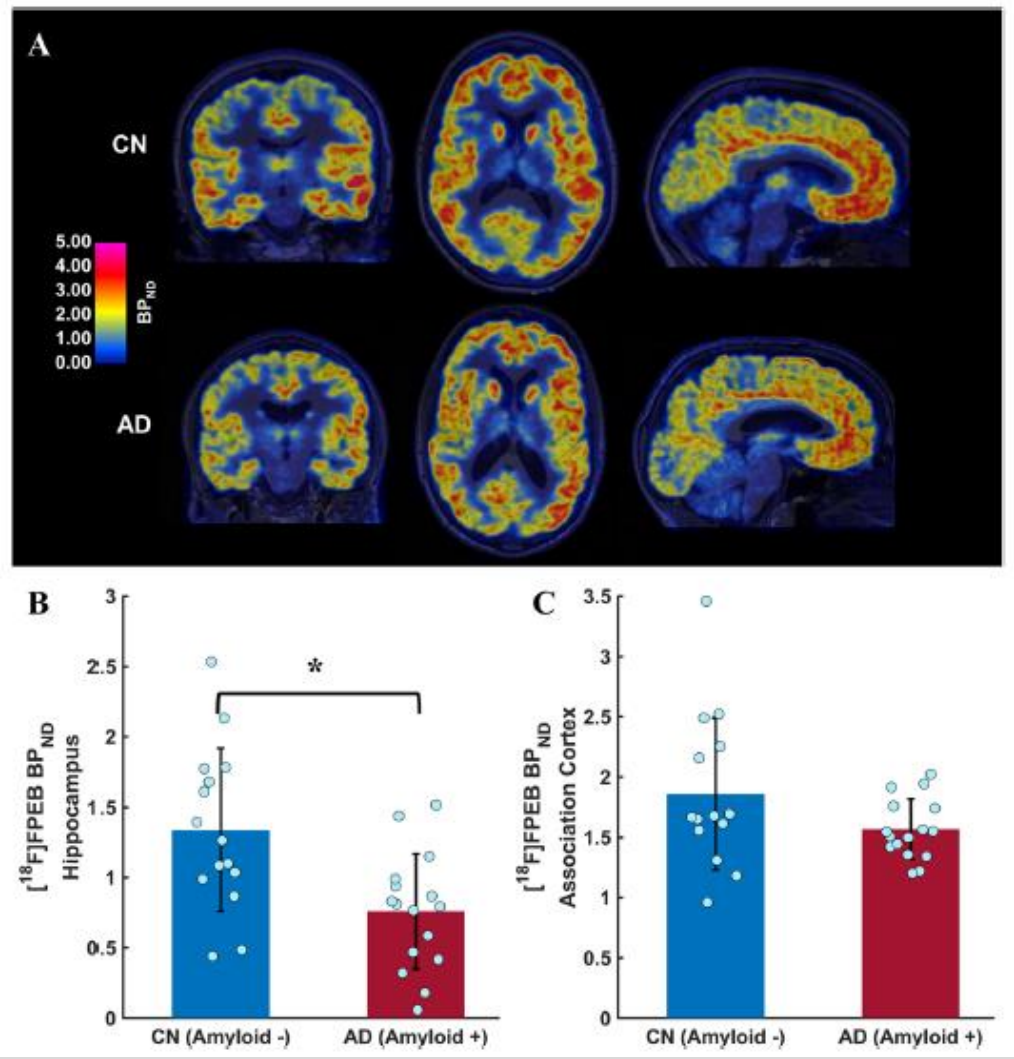

Decrease of hippocampal Metabotropic Glutamate Receptor5mGluR5 (both pre- and post synaptic)

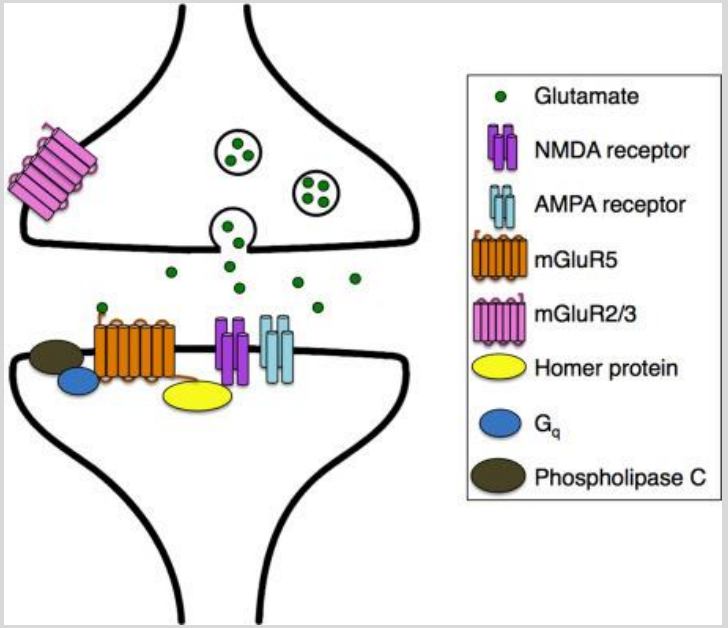

Mecca, 2020

Synaptic vesicles 2A (SV2A) protein

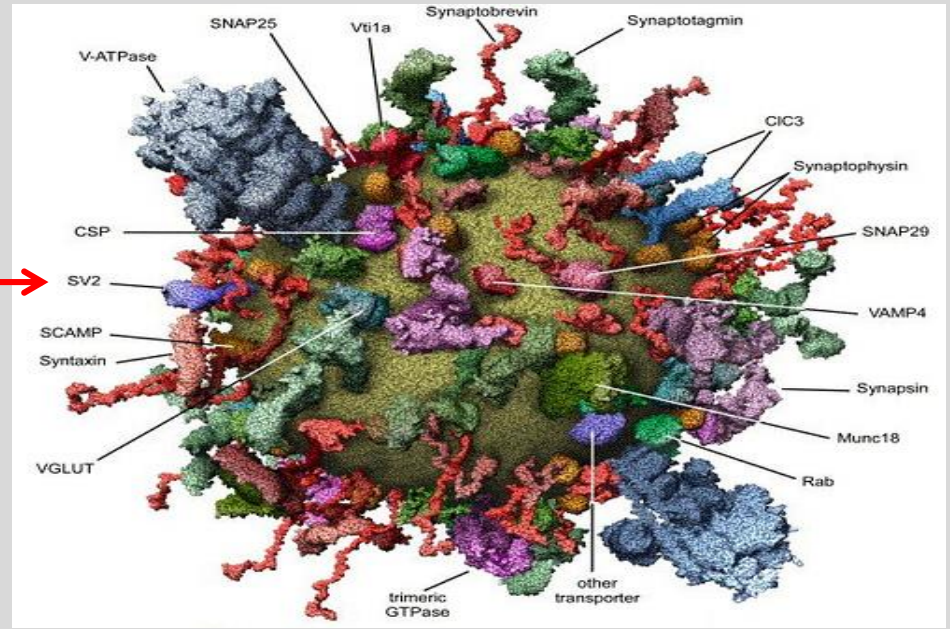

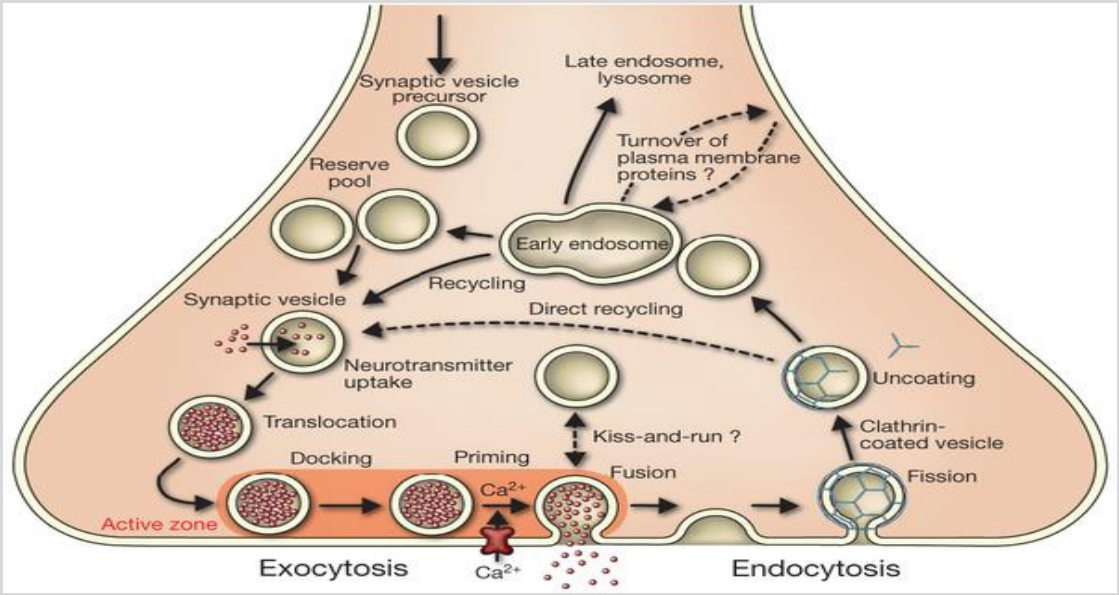

Radiotracer:
[18F]UCB-H

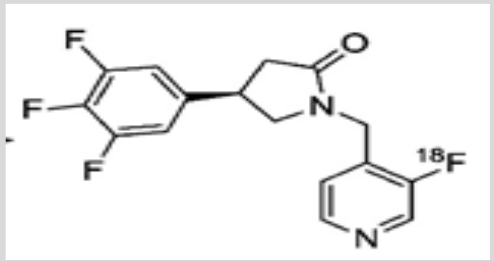

SV2A is involved in synaptic vesicle trafficking

SV2A is ubiquitous in the brain

SV2A-PET in AD

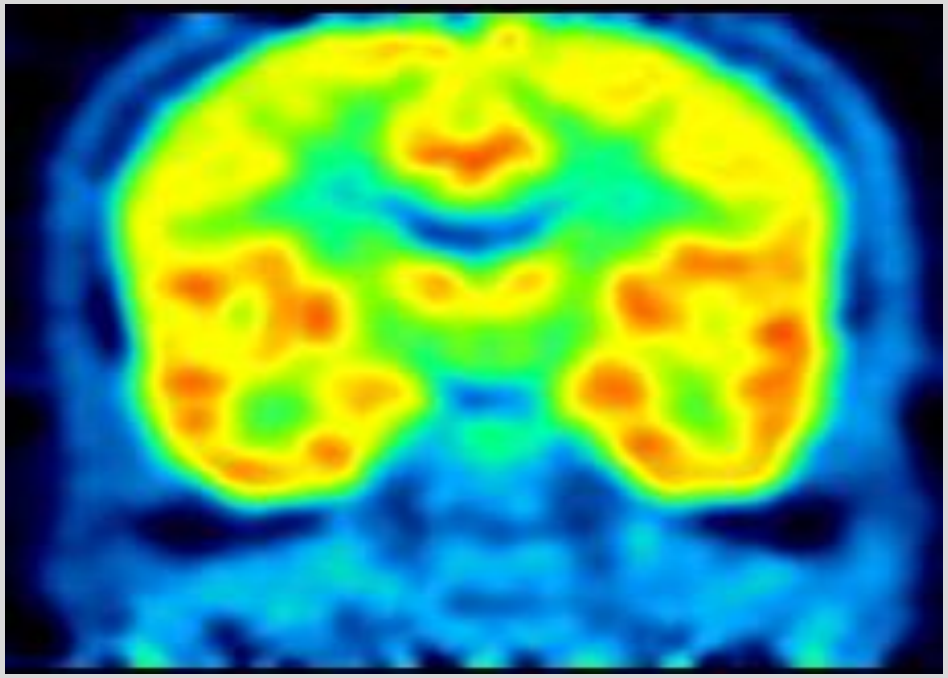

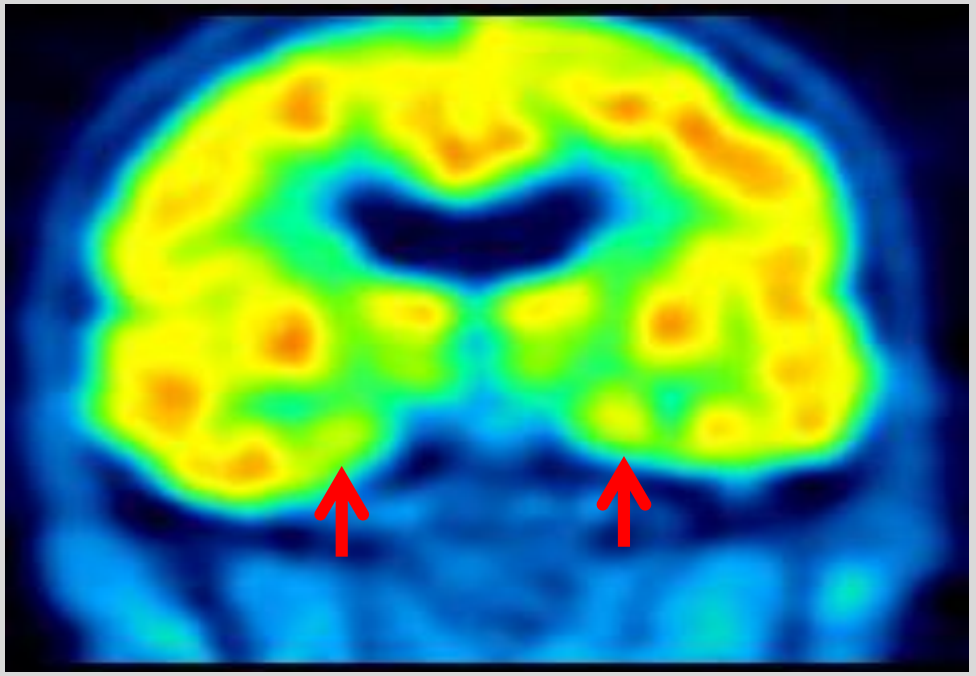

Control

Mild AD

Visual analysis suggest a decrease in SV2A binding in medial temporal structures

Bastin, EJNMMI 2019

SV2A & tau-PET in AD' s MTL

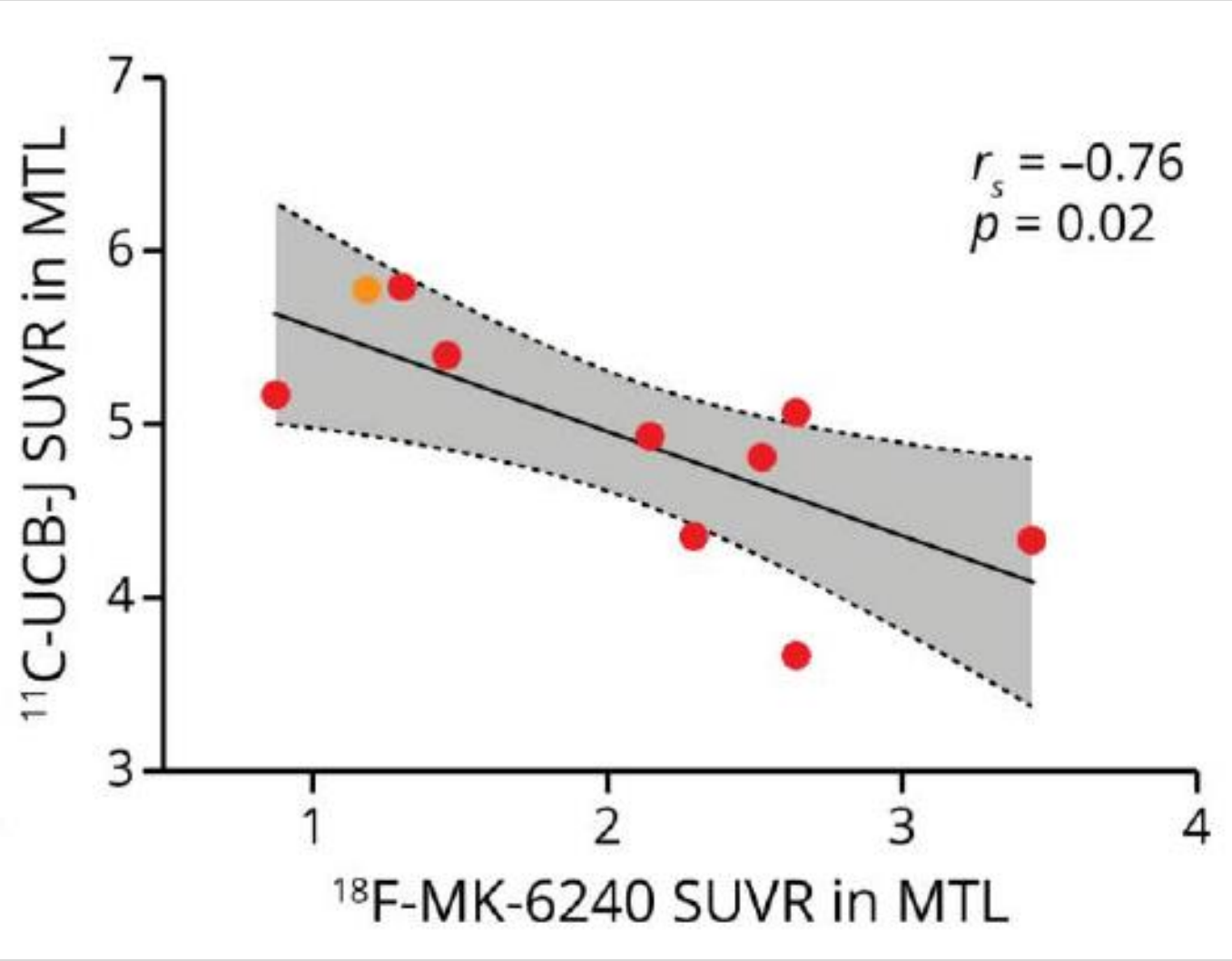

High correlation

(no causality)

Vanhaute et al, 2020

FrontoTemporal Lobe Degeneration

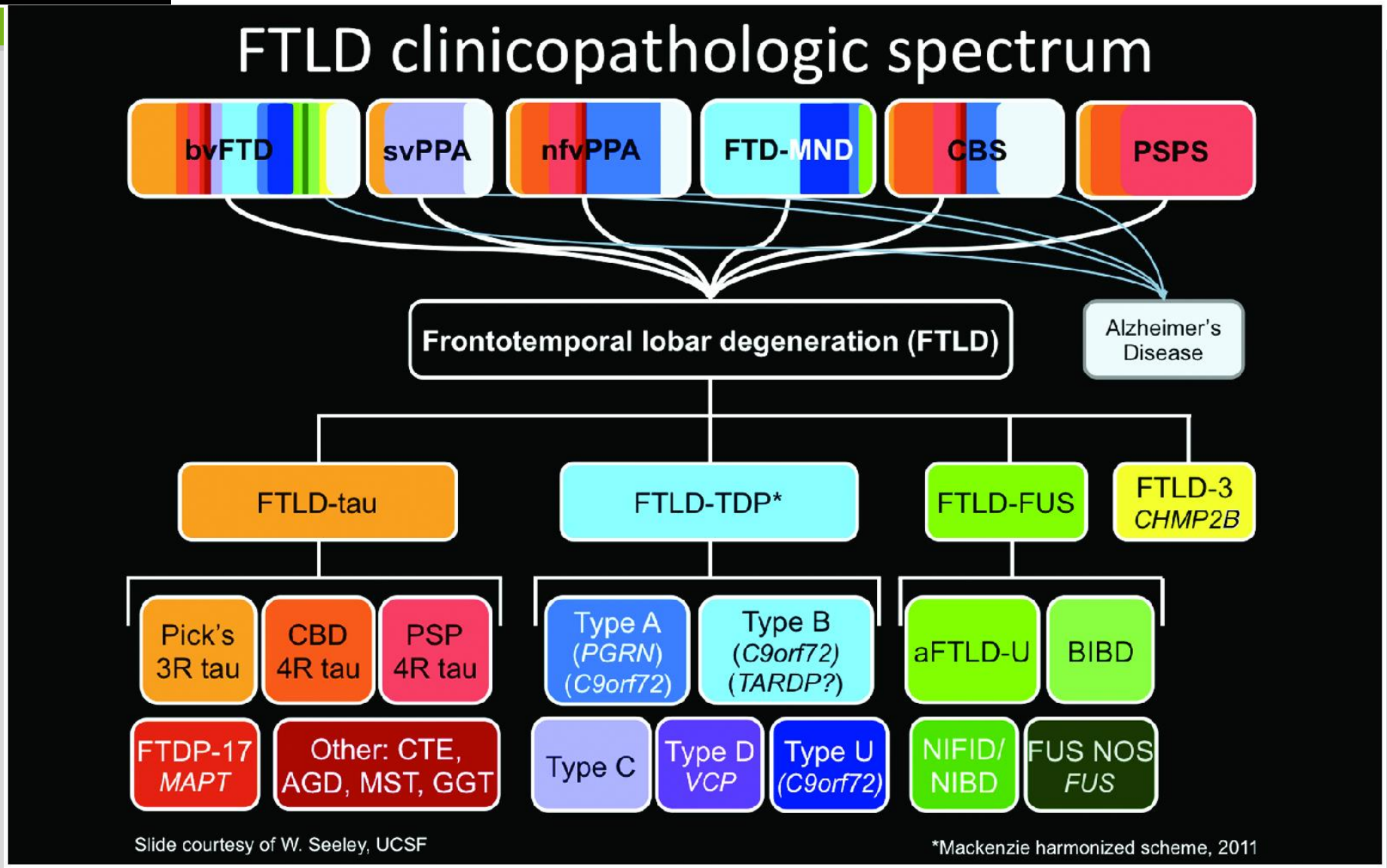

FrontoTemporal Lobe Degeneration

MOUSE MODELS

TDP-43
Motor changes
Behavioural
Memory

C9ORF72
Behavioral
Motor changes

TAU
Motor
Behavioural
Memory

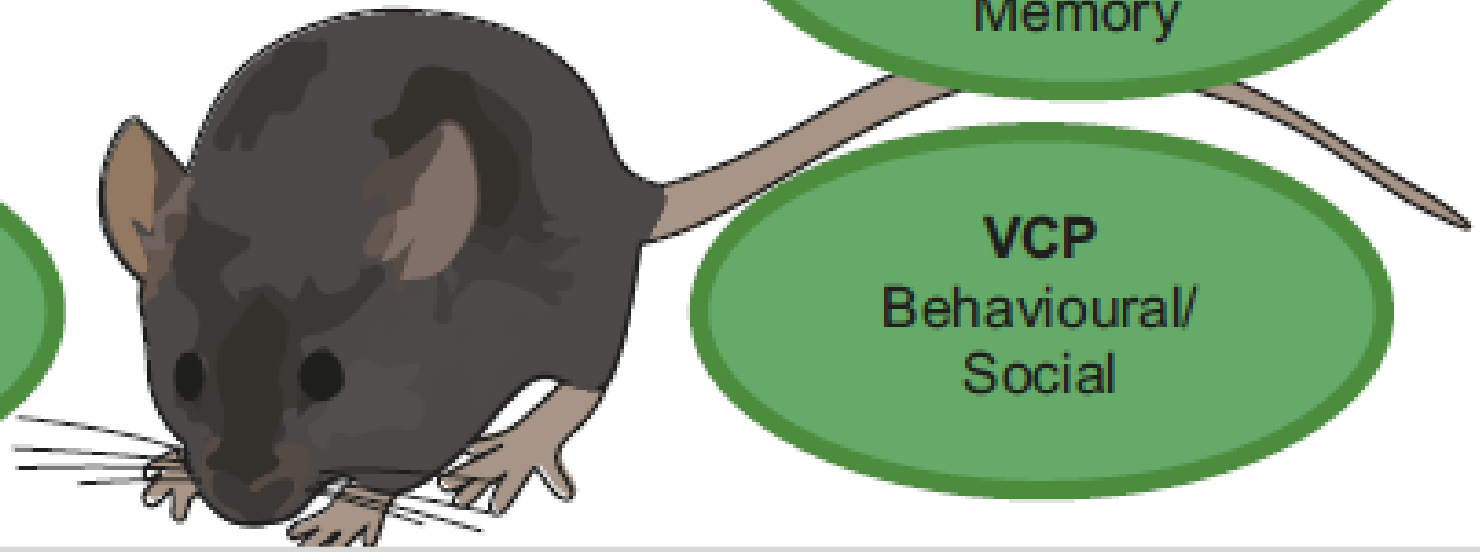

PROGRANULIN
Behavioural changes

VCP
Behavioural/
Social

Behavioral & social disturbances in bvFTD

Disinhibition

Apathy

Loss of empathy

Stereotyped behavior

Hyperorality

… and language in the other variants

FDG-PET in FTD

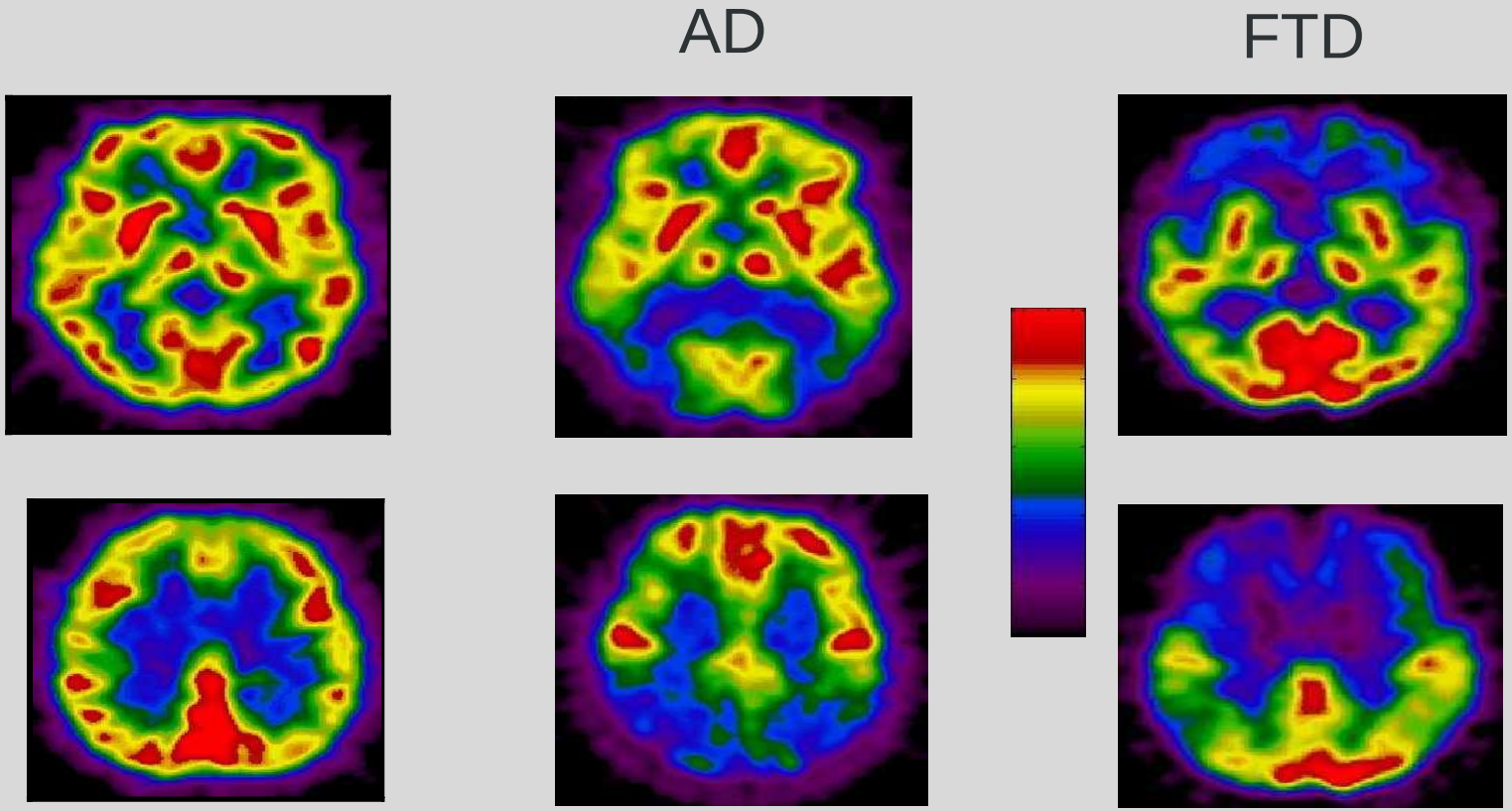

FDG-PET in FTD

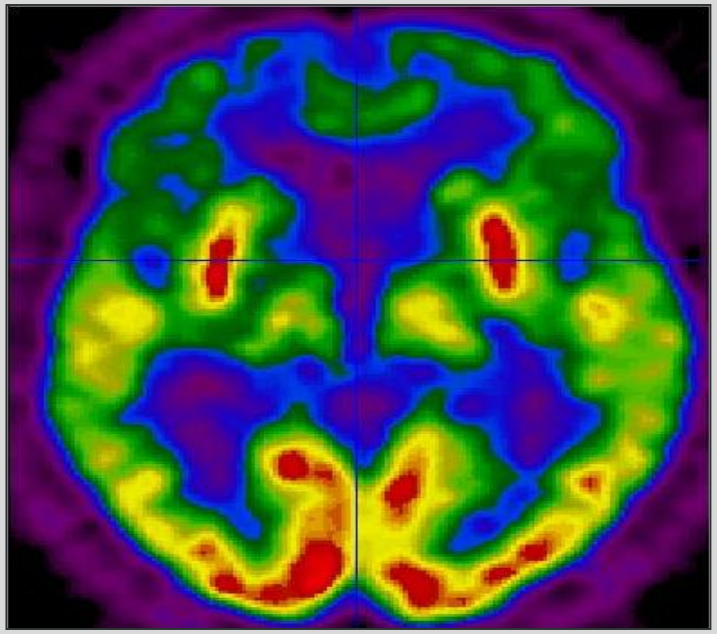

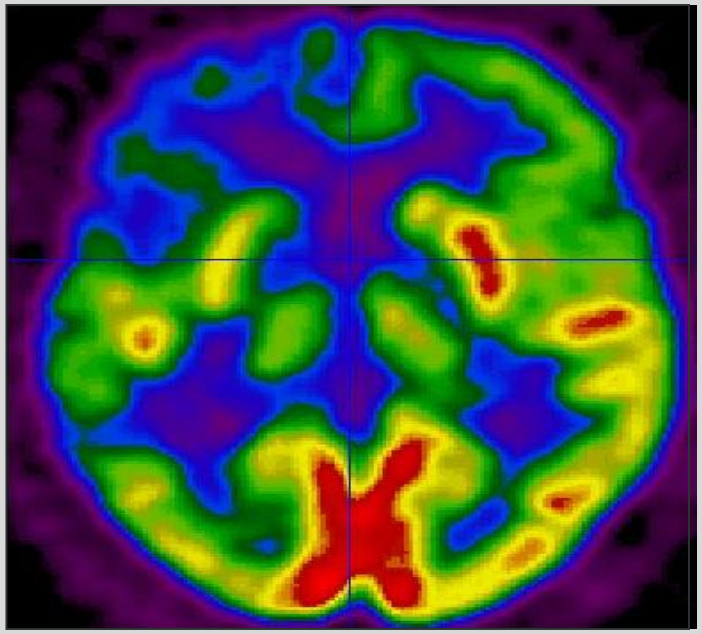

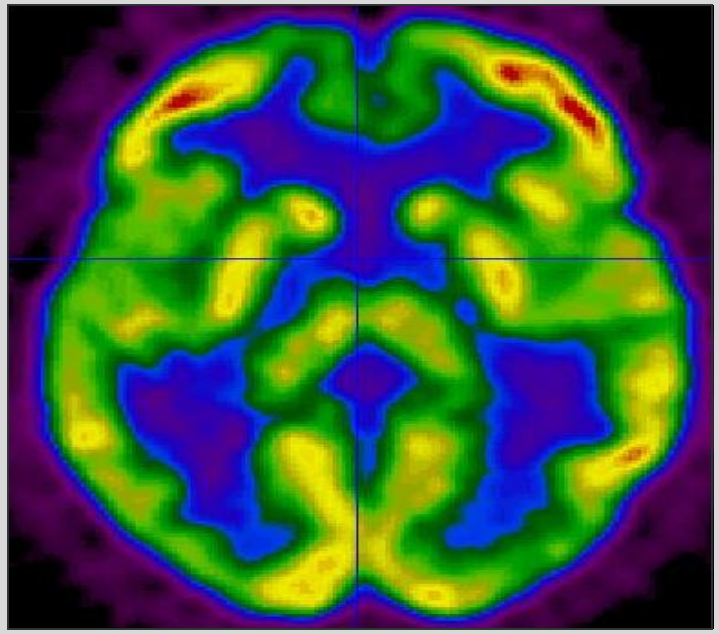

Variable involvement of frontal cortex

FDG-PET in temporal cortex of FTD

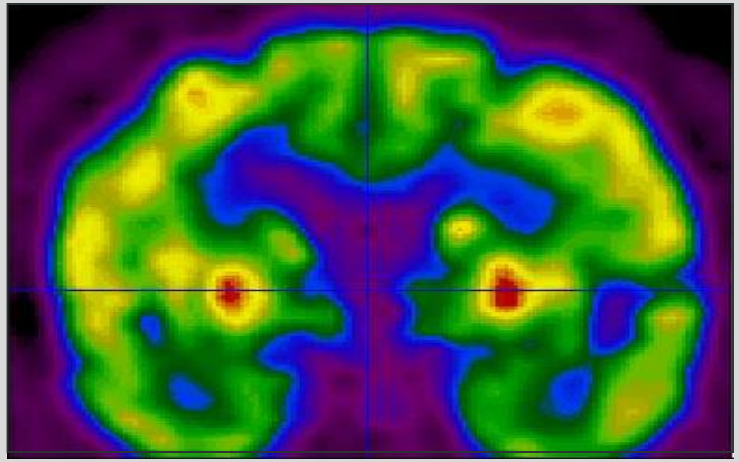
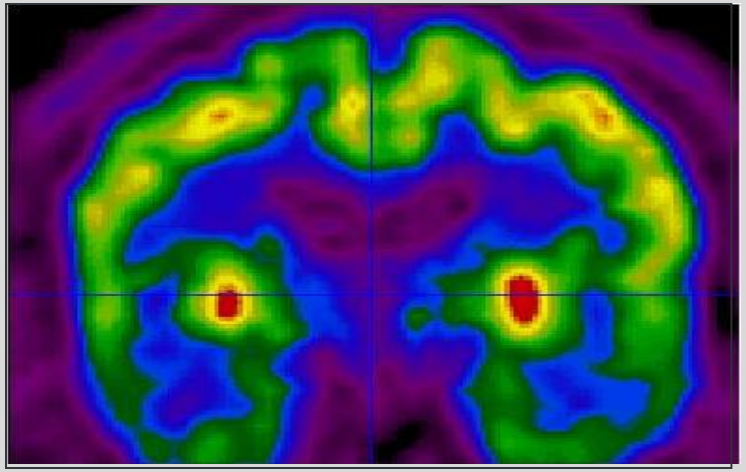
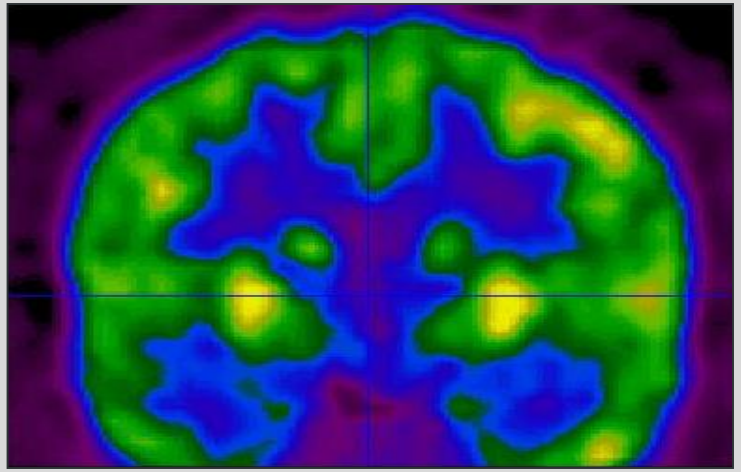
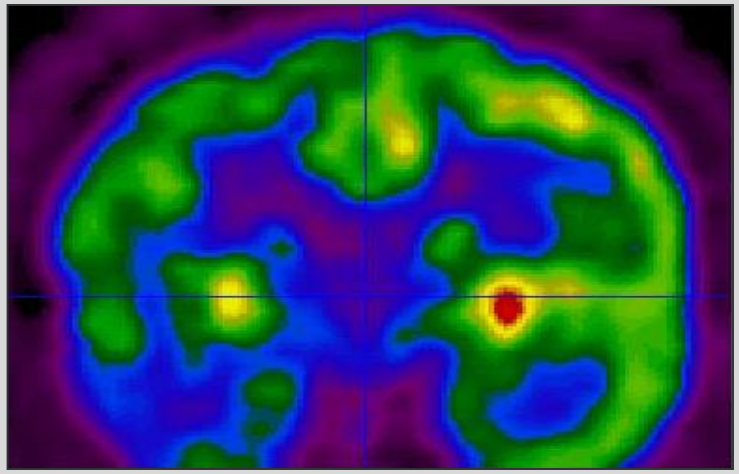
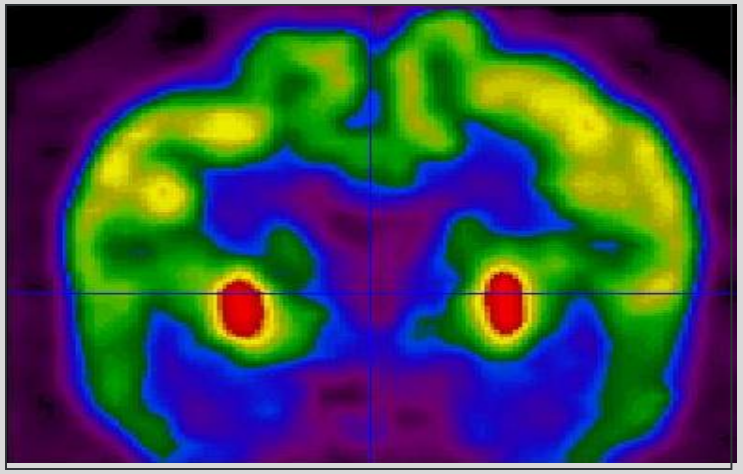
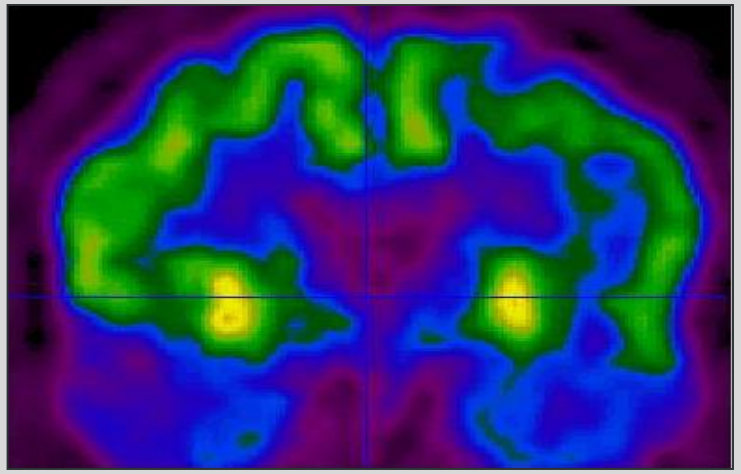

SV2A-PET in FTD's MTL

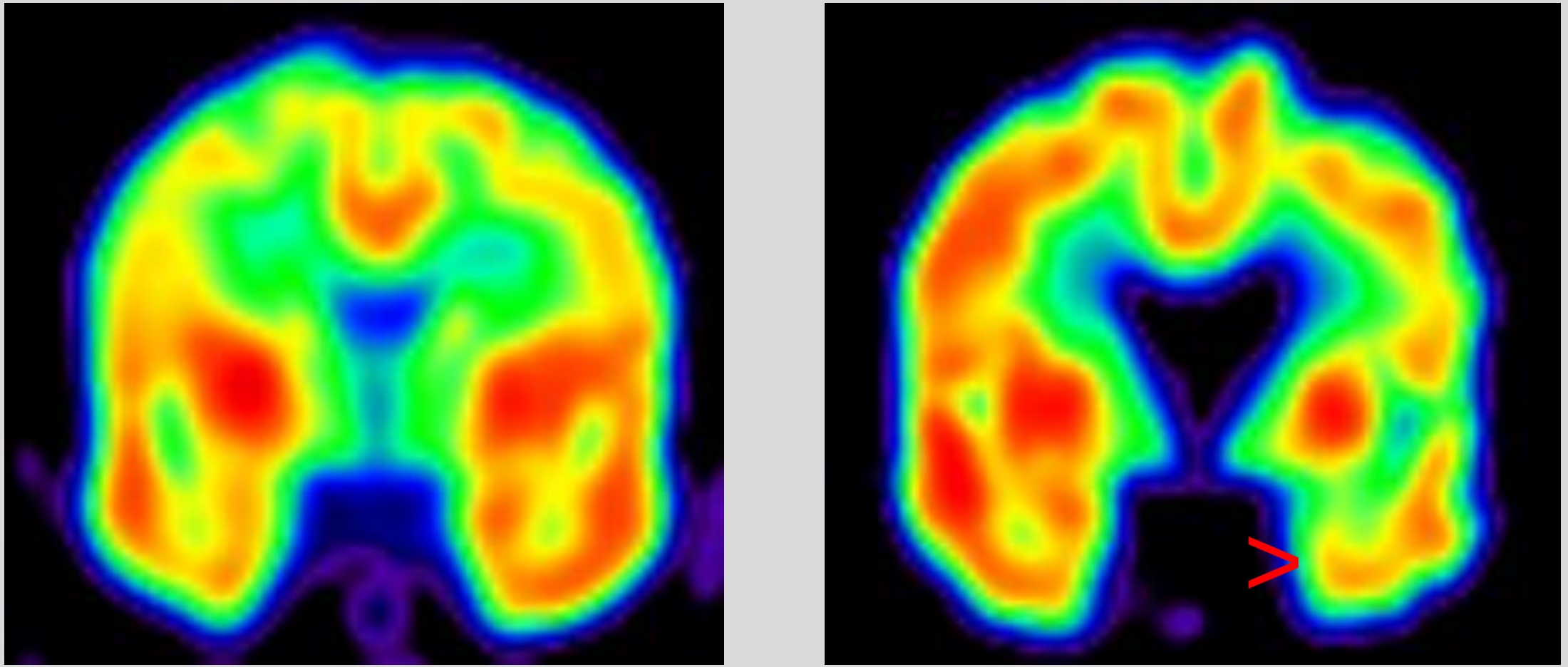

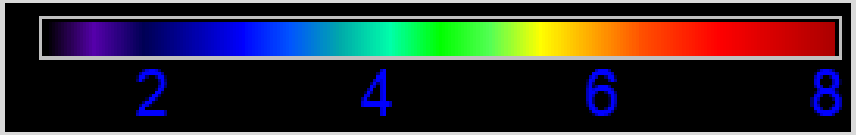

Tau-PET variability in FTD

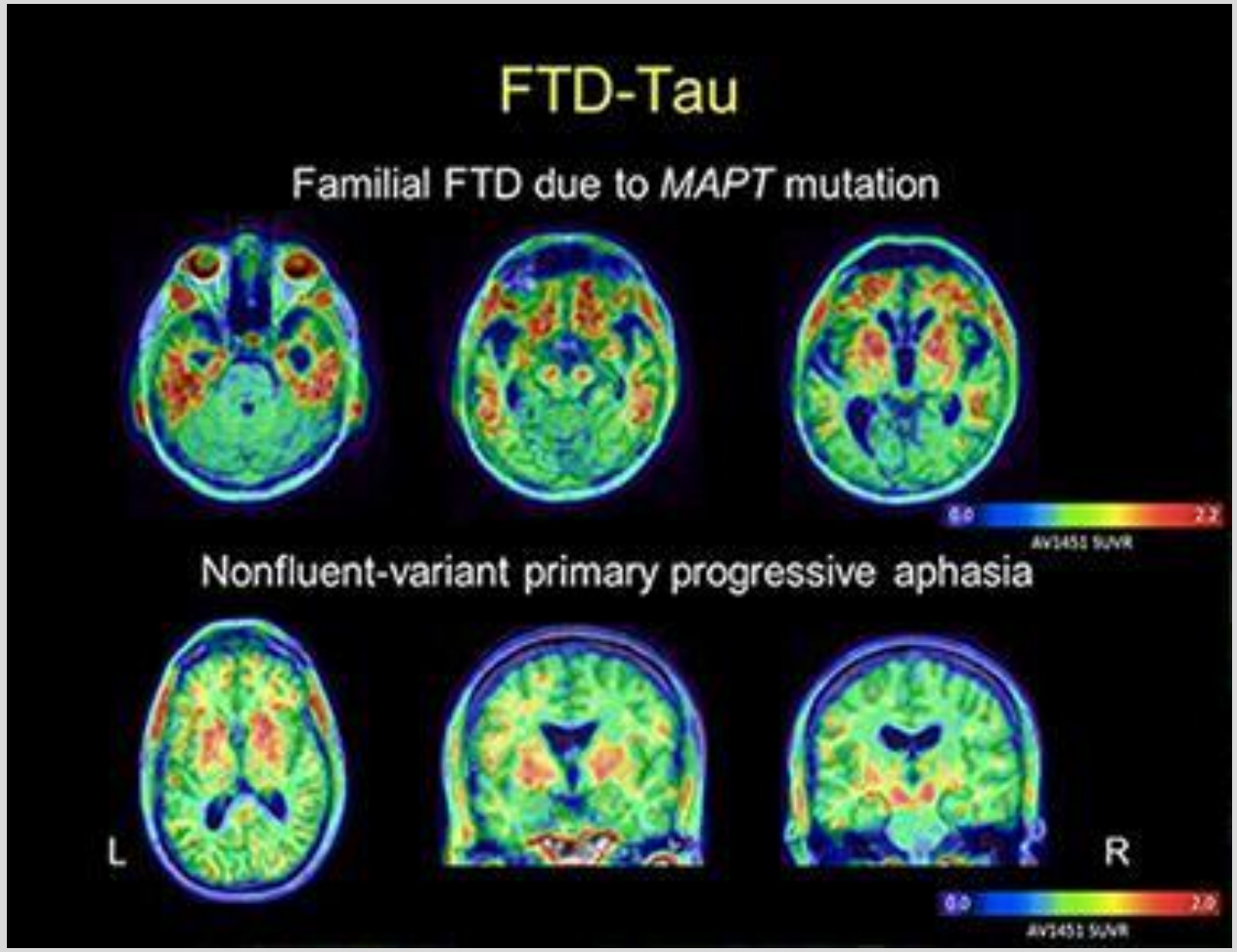

4R-Microtubule Associated Protein Tau

3R/4R-Microtubule Associated Protein Tau

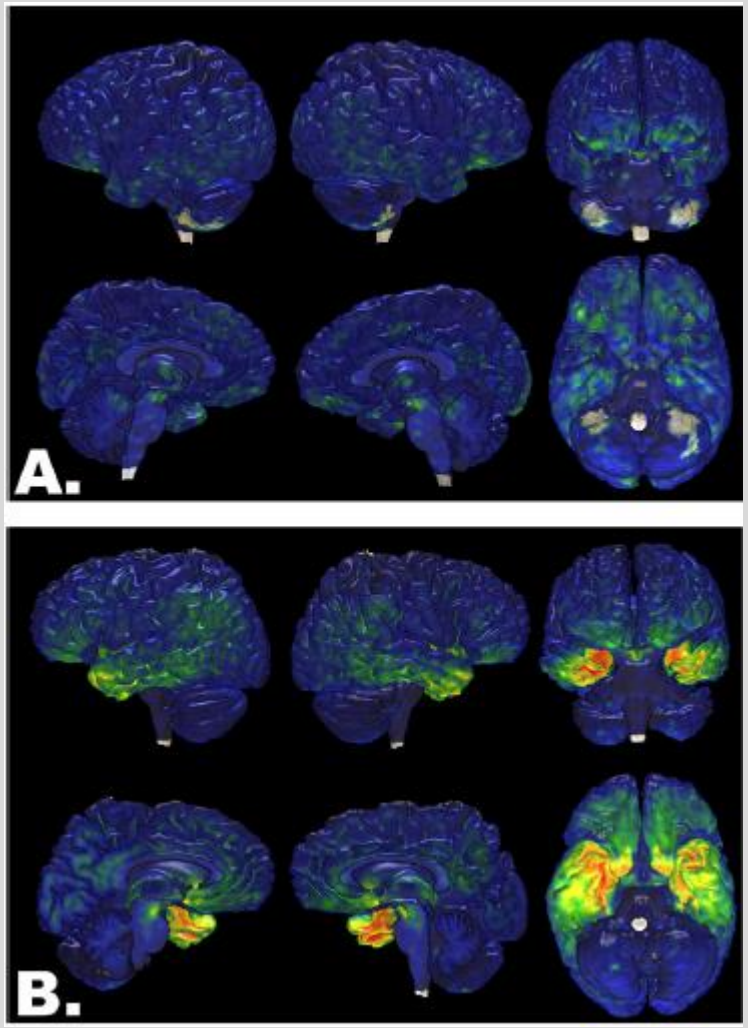

Whitwell, 2019

Tau-PET variability in bvFTD

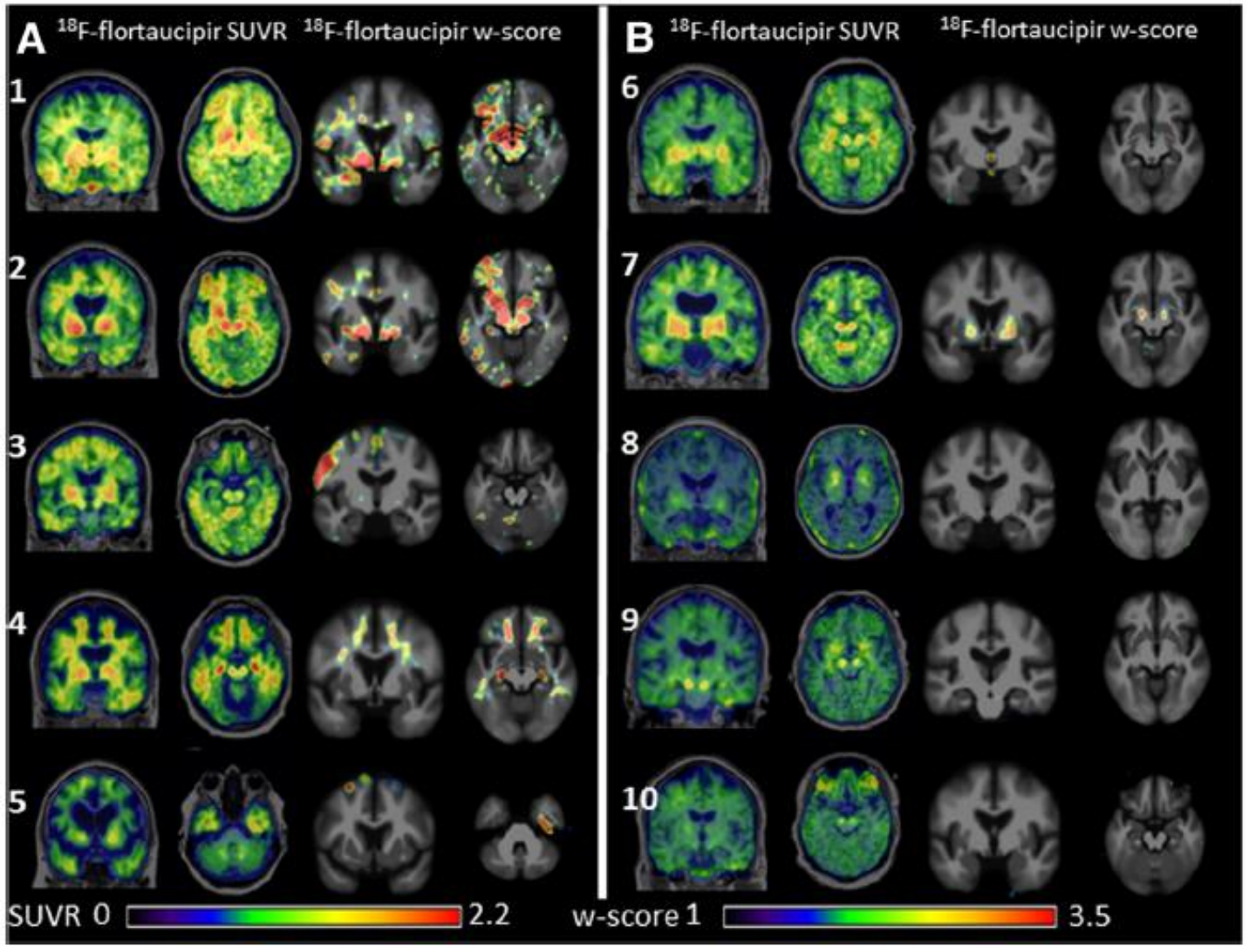

Tsai, 2019

Conclusion

Molecular imaging and biomarkers are key elements for new concepts of neurodegenerative diseases


G I G A


LIÈGE
université


CHU
de Liège


G I G A


Cyclotron
research centre